Johannes Kepler University Linz
Physical Chemistry

Time Resolved, Photoinduced Electron Spin Resonance Experiments on Conjugated Polymer/C$_{60}$ Composites

Diploma thesis

by

Markus C. Scharber

under the supervision of

O. Univ. Prof. Mag. Dr. N. Serdar Sariciftci

Linz, Austria, October 1998

Eidesstattliche Erklärung

Hiermit erkläre ich an Eides statt, die vorliegende Diplomarbeit selbstständig verfaßt, keine als die angegebenen Quellen und Hilfsmittel benutzt und mich auch sonst keiner unerlaubten Hilfe bedient zu haben.

Diese Diplomarbeit wurde bisher weder im Inland noch im Ausland als Prüfungsarbeit vorgelegt.

Linz, Österreich, Oktober 1998

Markus Clark Scharber

Abstract

In solid-state films of conjugated polymer - fullerene mixtures an ultrafast photoinduced charge transfer has been reported. An electron is transferred from the polymer to the fullerene leaving a positive polaron on the polymer chain. Both the transferred electron and the left positive polaron carry spin and therefore Electron Spin Resonance is the method of choice to investigate the charge-transfer states. In this work time resolved light induced electron spin resonance (TRLESR) studies and cw-light induced electron spin resonance studies on polymer fullerene mixtures are presented. After arranging the experimental set-up for TRLESR it was tested by investigating known reference systems. Experiments on conjugated polymers, fullerene mixtures in solution show that the photoinduced C_{60} triplet is influenced by the presence of the conjugated polymer. The triplet signal decay is much faster. Although electron transfer from the conjugated polymer to the fullerene can be observed in films by (near) steady state techniques (LESR, PIA) no ESR signal can be found in these systems using TRLESR technique. The missing electron polarisation effects which are essential for TRLESR or/and the nature of the photoinduced paramagnetic species can explain this result.

Contents

List of Figures

List of Tables

Chapter 1

Introduction and Outline

The discovery of highly luminescing conjugated polymers and the photo-induced electron transfer in solid state conjugated polymer fullerene composites has attracted considerable scientific and technological attention [1-4]. Light emitting diodes [5] based on conjugated polymers are waiting to be released to the market. A photovoltaic effect and non-linear optical properties have been demonstrated in polymer-fullerene mixtures [1]. Although people have already started working on devices (LED, solar cell, optical limiters) the nature of some of the excited states present in these systems is still controversial [6].

A lot of information about these photoinduced intermediate states can be gained by investigating their spin signature. The method of choice for these investigations is Electron Spin Resonance (ESR). To get additional information about the time evolution of the excited states, the time resolved (light induced)[1] electron spin resonance (TR(L)ESR) technique has been developed, starting with the work of Kim and Weissman [7-9]. TRLESR has been successfully be applied to photosynthectic reaction centers [10] and with its help, the primary events in photosynthesis have been clarified.

The central issue of the thesis is:

- arranging the set-up for TRLESR experiments around a Bruker ESR-spectrometer and a pulsed laser system
- testing the system

---

[1] In the literature the technique is often only called Time Resolved Electron Spin Resonance (TRESR) without specifying the way the excited particles are created.

- to investigate light induced excited states in conjugated polymer - fullerene composites

The main part of the thesis has been experimental work (setting up the system, design data acquisition programs, learn how the experiment has to be performed). Therefore a significant part of the report will be about the experiment.

Chapter 2 is dedicated to properties of conjugated polymers and fullerenes and to some characteristics of the charge transfer in these systems. In Chapter 3 the principles of time-resolved light induced electron spin resonance are described and a model for the interpretation of the experiments is discussed. At the beginning of chapter 2 and 3, the reader can find references in which a more thorough treatment of the topics can be found. Chapter 4 deals with the experimental set-up. In Chapter 5, experimental results are presented, showing that the set-up is working. In Chapter 6 first results of TRLESR experiments on conjugated polymer/fullerene composites are discussed. In the last chapter (7) a summary and acknowledgements can be found.

References

[1] N. S. Sariciftci, L. Smilowitz, A. J. Heeger and F. Wudl, Science, **258**: 1474, 1992

[2] N. S. Sariciftci, A. J. Heeger, Int. J. Mod. Phys. B8: 237, 1994

[3] N. S. Sariciftci, A. J. Heeger, in Handbook of Organic Conductive Molecules and Polymers, H. S. Nalwa (ed.), John Wiley&Sons, 1996

[4] N.S. Sariciftci, Prog. Quant. Electr., 19: 131, 1995

[5] J. H. Burroughes, D. D. C. Bradley, A. R. Brown, R. N. Marks, K. Mackay, R. H. Friend, P. L. Burn and A. B. Holmes, Nature 347 (1990) 539

[6] Primary Photoexcitations in Conjugated Polymers, N. S. Sariciftci (ed.) (World Scientific, Singapur, 1998)

[7] S.S. Kim, S. I. Weissman, Journal of Magnetic Resonance, 24: 167-169, 1976

[8] S.S. Kim, S. I. Weissman, Chemical Physics Letters, Vol. 58, 3: 326, 1978

[9] S.S. Kim, S. I. Weissman, Rev. Chem. Intermed. 3: 4380, 1979

[10] The Photosynthetic Reaction Centre, Vol. II, Chapter 12 & 13, J. Deisenhofer (ed), Academic Press (1993)

Chapter 2

Conjugated Polymers, Fullerenes, Charge Transfer

In this chapter fundamental concepts of conjugated polymers, fullerenes and the charge transfer from conjugated polymers to fullerenes are described. A more detailed treatment of conjugated polymers can be found in reference [1]. A comprehensive discussion on the science of fullerenes is given in reference [2]. Further details about charge transfer can be found in reference [3] and references therein.

Conjugated Polymers

Polymers are typically thought to be insulators and generally not to be considered as interesting electro-optic materials. This attitude has changed during the last three decades starting with the discovery of high electrical conductivity in polyacetylene [4]. Undoped conjugated polymers exhibit electronic and optical properties of a semiconductor in combination with the mechanical properties of polymers. By doping conductivities as high as 10^5 S/cm can be obtained [1]. The structures of some common conjugated polymers are shown in Fig. 2.1. Conjugated means that the backbone carbon chain is unsaturated and therefore has alternating double and single bonds. Hypothetically the electrons populating the p_z orbitals of the carbon atoms in a linear sp^2 carbon chain are delocalised and create a half-filled valence band. This would predict a metallic ground state for these materials (Fig. 2.2a). However 1-dimensional metals (quasi 1-dimensional) are not stable (Peierls transition) [5]. By distorting the spacing between the successive carbon atoms along the chain the system can gain energy. This dimerisation of the sp^2 hybridised carbon chain opens up an energy gap at the Fermi level and a semiconductor like electronic structure occurs

(Fig. 2.2b). There are two classes of conjugated polymers. The most prominent member of the so-called

trans-polyacetylene (PA)

polythiophene (PT)

polyparaphenlylene vinylene (PPV)

polyparaphenylene (PPP)

poly(3-octylthiophene) (P3OT)

poly(2-methoxy,5-(3',7'-dimethyloctyloxy)-
1,4-phenylenevinylene (MDMO-PPV)
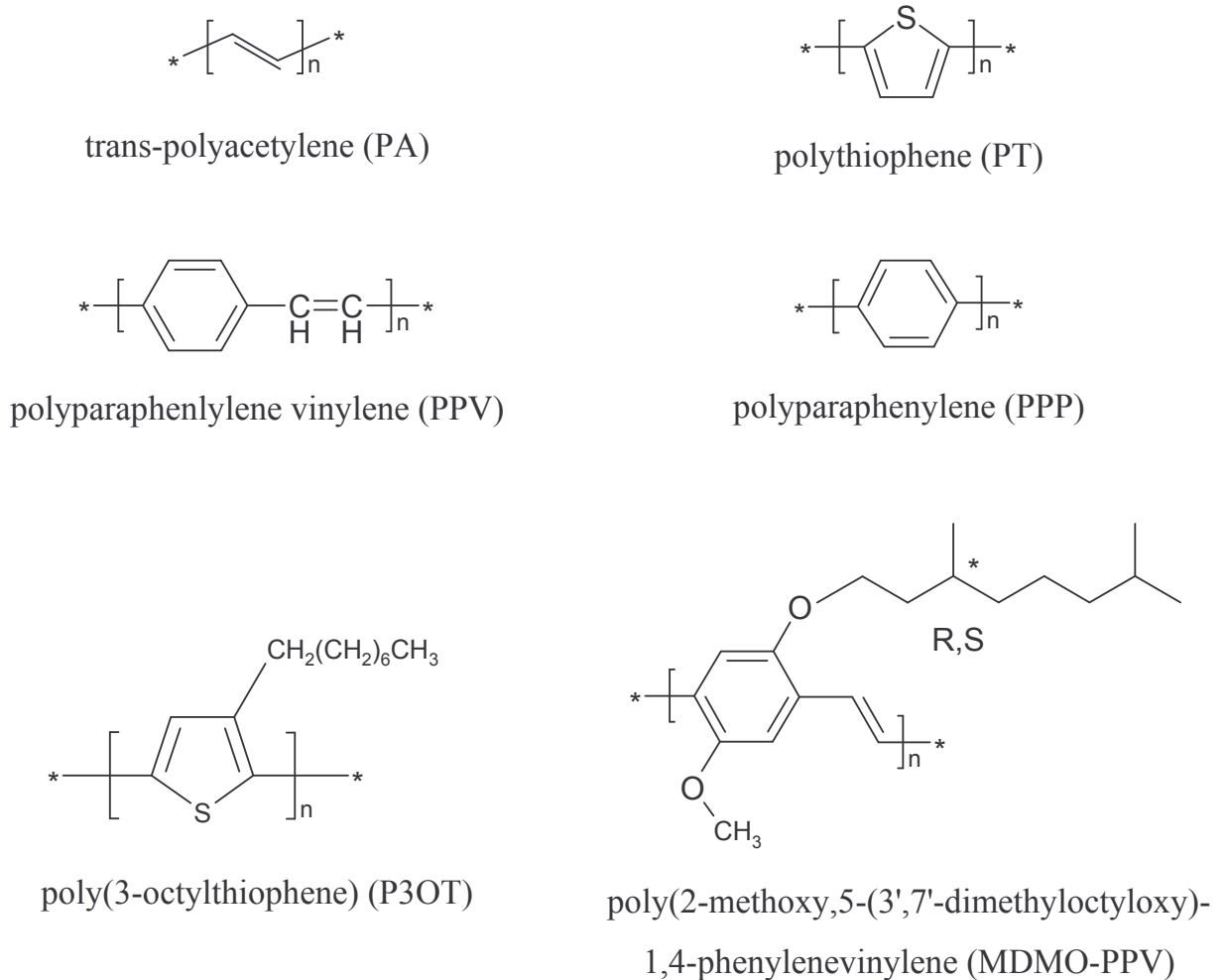
Figure 2.1: Examples for different conjugated polymers

degenerate ground state conjugated polymers is trans-polyacethylene. All the PPV's and POT's are members of the non-degenerate ground-state conjugated polymers. Degenerate means that the energy does not change when single and double bonds are interchanged. In non-degenerate materials different arrangements of single and double bonds are energetically different. Due to the 1-dimensional nature of the polymeric π-electrons (semiconducting) and the different structural properties (degenerate, non-degenerate) one can think of a variety of quasi-particles and excitations. Within the SSH (Su-Schrieffer-Heeger) Model [6][7] only solitons can be discussed. To include

polarons and bipolarons the SSH formalism has to be extended [7]. Each of these particles is delocalised over some repeating units of the polymer. If the two energetically equivalent phases (degenerate ground state) exist on a single chain the phase boundary between them is called a topological soliton, which can travel along the chain without changing its shape. Associated with each soliton is an electronic state with energy nearly at half of the energy gap. A neutral soliton (Fig. 2.3a) has
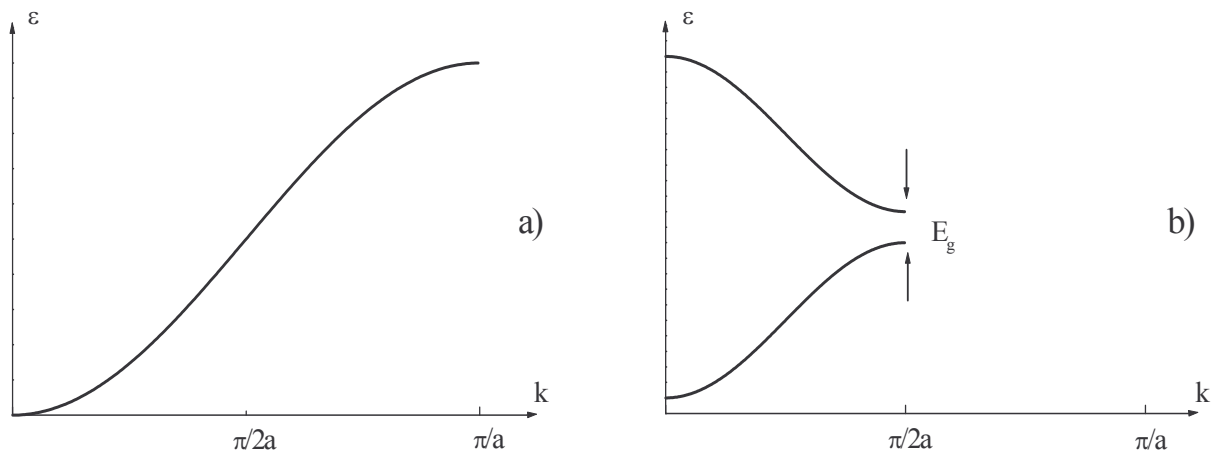
Figure 2.2: Schematic description on the Peierls transition. In a) the hypothetical metallic state is shown; b) the semiconducting bandstructure is illustrated

spin ½. Positively (Fig. 2.3b) and negatively (Fig. 2.3c) charged solitons have an unoccupied and doubly occupied mid-gap state respectively and no spin (spin-charge reversal). In non-degenerate polymers the soliton separates a low energy from a high-energy region and a soliton would be driven to the chain end minimising the total energy. However two defects can give rise to another quasi-particle in degenerate as well as
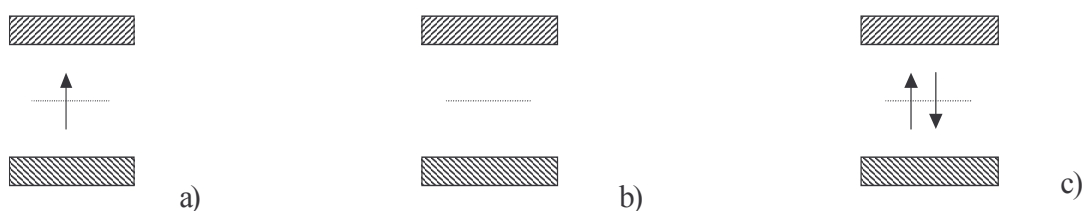
Figure 2.3: a) neutral soliton; b) positively charged soliton; c) negatively charged soliton

non-degenerate materials. Such double-defects are called polarons consisting of a neutral and a charged soliton. A polaron is characterised by two states in the gap (Fig. 2.4) and has charge and spin. One can also think that the mid-gap-states are completely empty or filled, corresponding to two positively or negatively charged solitons. The resulting particles are
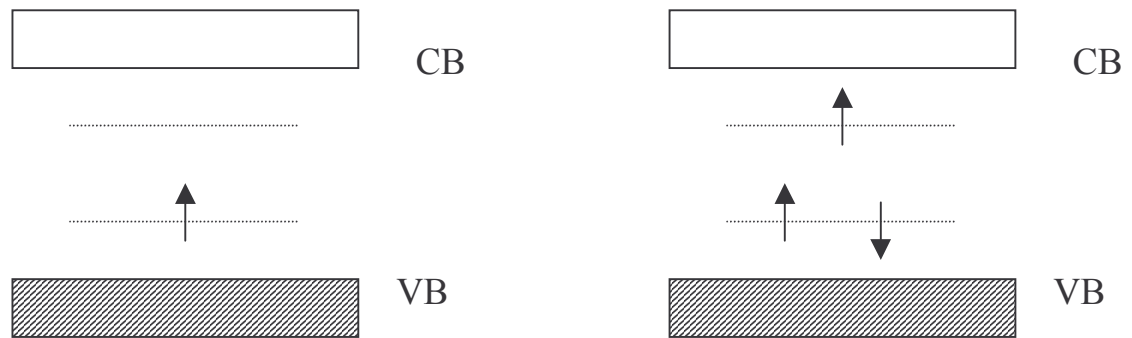
Figure 2.4: Positive and negative polarons

called bipolaron, since in case two polarons meet, the two neutral solitons form the bond and only the charged solitons are left over. A bipolaron has charge $\pm 2e$ but no spin. The concept of solitons and polarons is widely accepted, however the existence of photoinduced bipolarons in conjugated polymers is still controversial.

In conjugated polymers with a rigid backbone, lattice relaxations are not very dominant. Therefore these materials show dominantly excitonic excitations [8]. Excitons are well known from solid state physics. Compared to polarons they have no charge, but can have spin (triplet excitons).

The Fullerene C_{60} and its Derivatives

Since the discovery of a simple method to produce and separate fullerenes in macroscopic quantity [9], these molecules have been studied intensively. By definition a fullerene is a closed cage molecule containing only hexagonal and pentagonal faces. Using Euler's theorem for polyhedra, one can show that all fullerenes must have 12

pentagonal faces and the number of hexagonal faces is arbitrary. Therefore C_{60} consists of 12 pentagons and 20 hexagons and belongs to the symmetry group I_h. The high symmetry of C_{60} gives rise to unique properties. Due to the degeneracy of the lowest unoccupied molecular orbitals, C_{60} has a very high electron affinity and can accept up to 6 electrons [10]. Doping C_{60}-films
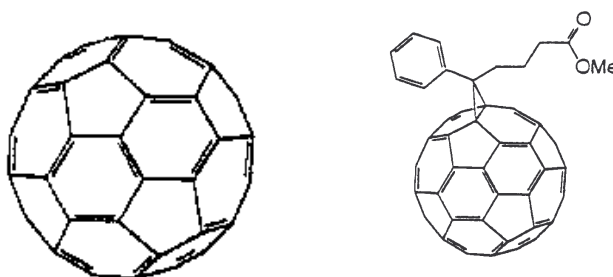
Figure 2.5: Structure of C_{60} and 1-(3-methoxycarbonyl)-propyl-1-phenyl-(6,6)C_{61} (PCBM) [11]

with some alkali-metals the material yields superconductivity at temperatures $T_c \geq 10K$ (high-temperature conductivity). C_{60} shows interesting mechanical properties and has also been used for drug-design [2].

To get higher C_{60} solubility in commonly used solvents, fullerene derivatives have been synthesised. Adding certain side-groups to the fullerene causes only small changes in the electronic structure but gives better processible materials.

Photoinduced Electron Transfer from Conjugated Polymers to Buckminsterfullerene

A basic description of an intramolecular and/or intermolecular photoinduced charge transfer process is as follows:

Step 1 : $D + A \rightarrow {}^{1,3}D^* + A$ (excitation of D);

Step 2: ${}^{1,3}D^* + A \rightarrow {}^{1,3}(D.....A)^*$ (excitation delocalised on D-A complex);

Step 3: ${}^{1,3}(D.....A)^* \rightarrow {}^{1,3}(D^{\delta+}.....A^{\delta-})^*$ (charge transfer initiated);
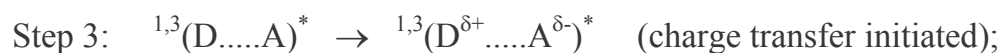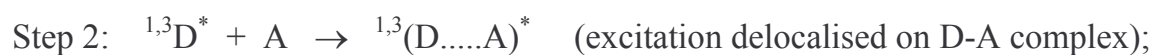
Step 4: $^{1,3}(D^{\delta+}.....A^{\delta-})^*$ $\rightarrow$ $^{1,3}(D^{+\bullet}.....A^{-\bullet})^*$ (ion radical pair formed);

Step 5: $^{1,3}(D^{\bullet+}.....A^{-\bullet})^*$ $\rightarrow$ $(D^{+\bullet} + A^{-\bullet})$ (charge separation);

where the donor (D) and acceptor (A) are either covalently bound (intramolecular) or spatially close but not covalently bonded (intermolecular). 1,3 indicates that the excited state (symbolised by *) can be in the singlet or the triplet state. A necessary but not sufficient condition for step 4 to occur is $I_D^* - A_A - U_C < 0$, where I_D^* is the ionisation potential of the excited state D^* of the donor, A_A the electron affinity of the acceptor and U_C the Coulomb energy of the separated radicals (including polarisation effects). The charge-separated state can be stabilised by carrier delocalisation on the donor and/or on the acceptor, by structural relaxation or by polarisation effects in highly polar environments (Marcus theory) [12].

The photoinduced electron transfer reported in C_{60}/conjugated polymer mixtures is reversible and one of the fastest ever reported (transfer occurs within ps) [13]. Clear evidences for the electron transfer in these systems are:

- almost complete quenching of the polymer luminescence and the polymer as well as C_{60} triplets

- observation of two light-induced ESR lines assigned to the polymer cation radical (positive polaron) and to the fullerene anion radical

- enhancement of photoconductivity by adding small amount of C_{60} to a conjugated polymer

- appearance of distinct features in time resolved and near steady-state photoinduced absorption measurements on conjugated polymer/C_{60} compounds, clearly showing the positive polaron on the polymer and the fullerene anion

References

[1] Handbook of Conducting Polymers, volumes 1&2 (Marcel Dekker, New York 1986)

[2] Science of Fullerenes and Caron Nanotubes, M.S. Dresselhaus, G. Dresselhaus, P. C. Eklund, Academic Press (1996)

[3] see N.S. Sariciftci, A.J. Heeger, Handbook of Organic Conductive Molecules and Polymers. Vol. 1 Charge-Transfer Salts, Fullerenes and Photoconducters. Edited by H.S. Nalwa, John Wiley & Sons Ltd 1997 and references therein

[4] H. Shirakawa, E.J. Louis, A.G. MacDiamid, C.K. Chiang and A. Heeger, Chem. Comm. 578 (1977)

[5] R.E. Peierls, Quantum Theory of Solids (Clarendon, Oxford 1955)

[6] A.J. Heeger, S. Kivelson, J.R. Schrieffer, W.-P. Su, Rev. of Modern Physics Vol. 60, No.3, 781, (July 1988)

[7] Y. Lu, Solitons and Polarons in Conducting Polymers (World Scientific, Singapore 1988)

[8] Primary Photoexcitations in conjugated polymers, N. S. Sariciftci, World Scientific, Singapore, 1998

[9] W. Krätschmer, D. Lamb, K- Fostiropoulos, D.R. Huffman, Nature, 347, 354, (1990)

[10]   P.-M. Allemand, A. Koch, F. Wudl, Y. Rubin, F. Diedrich, M.M. Alvarez, S.J. Anz and R.L. Whetten, J. Am.Chem. Soc. 113, 4364 (1991)

[11]   J. C. Hummelen, B. W. Wright, F. Lepel, F, Wudl, J. Org. Chem. 60(1995) 532

[12]   Marcus R. A.: Ann. Rev. Phys. Chem. 15., 155(1964)

[13]   N.S. Sariciftci, L. Smilowitz, A.J. Heeger, F. Wudl, Science Vol.258, 1474, 1992

Chapter 3

Time Resolved Light-Induced Electron Spin Resonance (TRLESR)

In this chapter the principles of TRLESR will be discussed. More detailed description can be found in references [1][2].

3.1 Basics of ESR Spectroscopy

Resonant absorption of electromagnetic radiation by paramagnetic species is called electron spin resonance. In almost all ESR experiments the degeneracy of the different paramagnetic eigenstates is lifted by an external magnetic field. The simplest energy-level diagram for a particle of spin ½ in a magnetic field is shown in Fig. 3.1.
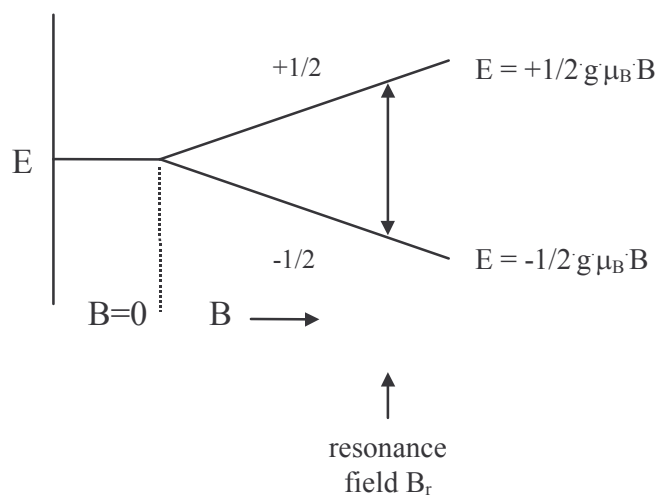
Figure 3.1: Energy-level scheme for a simple system (one single spin 1/2) as a function of the applied magnetic field B. The constants g and μ_B are defined in the text below

By varying the static field B, one may change the energy-level separation (Zeeman splitting), as indicated. Resonant absorption occurs if the frequency is adjusted so that $\Delta E = h \cdot \nu$. Here ν is the frequency of the incident electromagnetic radiation and ΔE is given by

$$\Delta E = g \cdot \mu_B \cdot B \qquad\qquad (3.1)$$

where g is the so called Lande-factor of the particle, which is one of the characteristic parameters representing the particle, μ_B is the Bohr magneton and **B** the external magnetic field (magnetic inductance) chosen to be along the z direction. The term 'magnetic field' (meaning **B**) is in almost universal usage in magnetic resonance. Hence I will continue to use the term magnetic field for the quantity B in the following parts of this manuscript.

3.2 The Philosophy of the TRLESR Technique

In steady-state continuous ESR the transitions are affected by sweeping an external magnetic field through each resonance at constant microwave frequency. The external magnetic field is modulated, usually at a frequency of 100 kHz , so that phase-sensitive detection can be used to increase the signal-to-noise (S/N) ratio significantly. A consequence of the 100 kHz field modulation is that the time response of the spectrometer becomes limited to, at best, the inverse of the modulation frequency. Practically, for good S/N, a few cycles of the modulation are necessary, which means that species with lifetime less than about 100 μs become difficult to detect. Another way to use ESR-spectroscopy to investigate short-lived paramagnetic particles would be sweeping the external magnetic field sufficiently rapid. Due to the inductance of the coils this method can not be used for sub-microsecond time resolution experiments.

Time resolution in TRLESR experiments is obtained by the following procedure. Pulses of light produced by a pulsed light-source (laser) illuminate the material under investigation. The pulse duration has to be comparable (or shorter) to the time-resolution of the experiment. No magnetic field modulation is used. The time evolution of the microwave intensity reaching the detector (e.g. microwave diode of the spectrometer) is monitored following each light pulse. The resolution is limited by the instrumental response i.e. bandwidth of the amplifiers or the response of the

microwave system and can be as low as 10 ns for an X-band (9.5 GHz) spectrometer [3].

In normal (cw) ESR, the spectra have intensities that reflect the relative populations of the energy levels as determined by the Maxwell-Boltzmann distribution. However, when the paramagnetic particles are created instantaneously within the magnetic field, they would not immediately be expected to be in thermal equilibrium. Polarisations of 10-100 times the equilibrium polarisation have been observed in experiments.

3.3 Theoretical Description of a TRLESR Experiment

In time-resolved light-induced ESR paramagnetic particles are created with their spins aligned with the magnetic field and this causes an initial magnetisation $M_z(0)$ in this direction. This is acted upon by the microwave radiation field, which rotates it to produce an orthogonal component $M_y(t)$, to which the observed signal is proportional. The signal initially increases as $M_y(t)$ grows under the rotation, but then it decays by relaxation and recombination. The analysis of the transient signals can be carried out using the Bloch equation

$$\frac{d\vec{M}}{dt} = \gamma \cdot \vec{M} \times \vec{B}$$

(3.2)

where $\vec{M}$ is the bulk magnetisation, γ the electronic magnetogyric ratio and $\vec{B}$ the acting magnetic field. Introducing the standard relaxation times T_1 (spin-lattice relaxation) and T_2 (spin-spin relaxation) and transforming to a rotating co-ordinate frame rotating about the z direction at the angular frequency of the microwave (ω) with the same sense as that of B_1

$$\frac{dM_x}{dt} = -\left(\omega_B - \omega\right) \cdot M_y - \frac{M_x}{T_2}$$

$$\frac{dM_y}{dt} = \left(\omega_B - \omega\right) M_x + \gamma \cdot B_1 \cdot M_z - \frac{M_y}{T_2} \qquad (3.3)$$

$$\frac{dM_z}{dt} = -\gamma \cdot B_1 \cdot M_y - \frac{M_z}{T_1}$$

is obtained [4].

The static field B is taken to have only a z component and an oscillating magnetic field B_1 (microwave) is imposed in a direction perpendicular to B.

$$B_{1x} = B_1 \cdot \cos(\omega \cdot t)$$
$$B_{1y} = B_1 \cdot \sin(\omega \cdot t) \qquad (3.4)$$
$$B_{1z} = 0$$

In the absence of spin polarisation, but with chemical reactions occurring, the Bloch equation may be written in the matrix form [1]

$$\frac{d\vec{M}}{dt} = \mathbf{L}\vec{M}(t) + T_1^{-1}\vec{M}_{eq}(t) - T_c^{-1}(t)\vec{M}(t) \qquad (3.5)$$

where it is assumed that the instantaneous value $M_z(0)$ relaxes toward its equilibrium value within a particular time t. $T_c(t)$ is the instantaneous lifetime of the radical, whose concentration is n(t) at this time and is given by the equations

$$T_c^{-1}(t) = \frac{\dot{n}(t)}{n(t)} \qquad (3.6)$$

and

$$\dot{n}(t) = -k_1 n(t) - k_2 \left[n(t)\right]^2 \qquad (3.7)$$

where k_1 and k_2 are pseudo-first-order and second-order rate constants. The matrix $\mathbf{L}$ can be extracted from above and is given by

$$L = \begin{bmatrix} -T_2^{-1} & \Delta\omega & 0 \\ -\Delta\omega & -T_2^{-1} & \omega_1 \\ 0 & -\omega_1 & -T_1^{-1} \end{bmatrix} \qquad (3.8)$$

$\Delta\omega$ is the offset from the resonance frequency and ω_1 is the microwave field strength given by γB_1 both measured in angular frequency units. $\mathbf{M}_{eq}(t)$ is given by

$$\vec{M}_{eq}(t) = n(t) \cdot P_{eq} \cdot \begin{bmatrix} 0 \\ 0 \\ 1 \end{bmatrix} \qquad (3.9)$$

where P_{eq} is the spin polarisation at thermal equilibrium.

General solutions of this set of differential equations can only be obtained using numerical computational techniques.

Predictions of these equations are shown in Fig. 3.2 [1], which portrays decay curves calculated for a given particle exactly on resonance at a series of microwave intensities (ω_1 values). At low microwave field strength the curve appears close to exponential. At
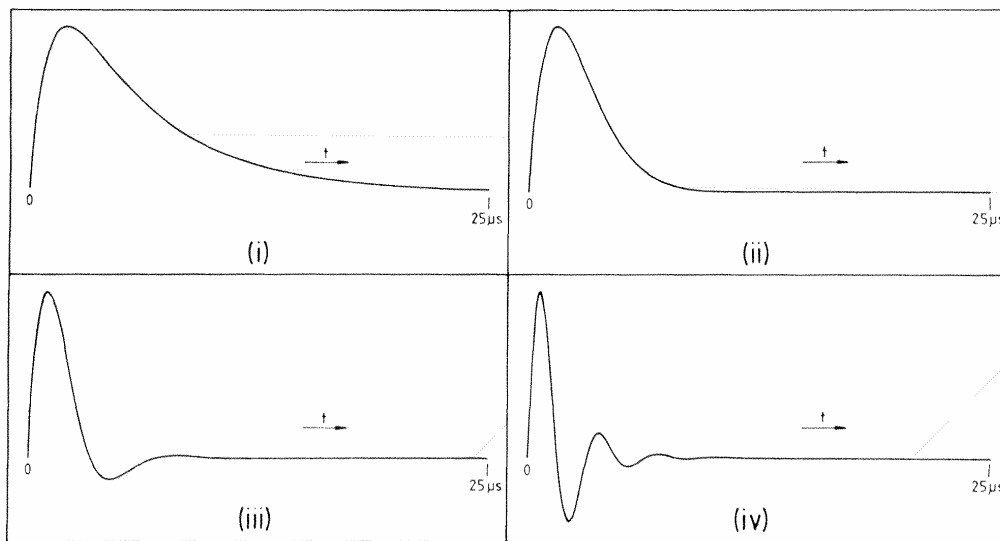
Figure 3.2: Decay curves calculated exactly on resonance for a radical with T_1=5 µs and T_2=1 µs, and with a microwave fieldstrengths ω_1 of (i) 0.01, (ii) 0.05, (iii) 1.0 and 2.0 rad MHz [1].

higher ω_1 values damped oscillations appear, becoming more pronounced as the value increases. This phenomenon is called transient nutation.

One can calculate the time-dependence of the ESR-signal observed after the radical creation with the magnetic field of the spectrometer set to a single chosen value. Repeating this calculation for a series of discrete values of the magnetic field then

allows a two-dimensional plot of the signal versus time along one axis and field along the other (Fig. 3.3). This calculation also yields the line-shape observed at any specific time after particle creation.
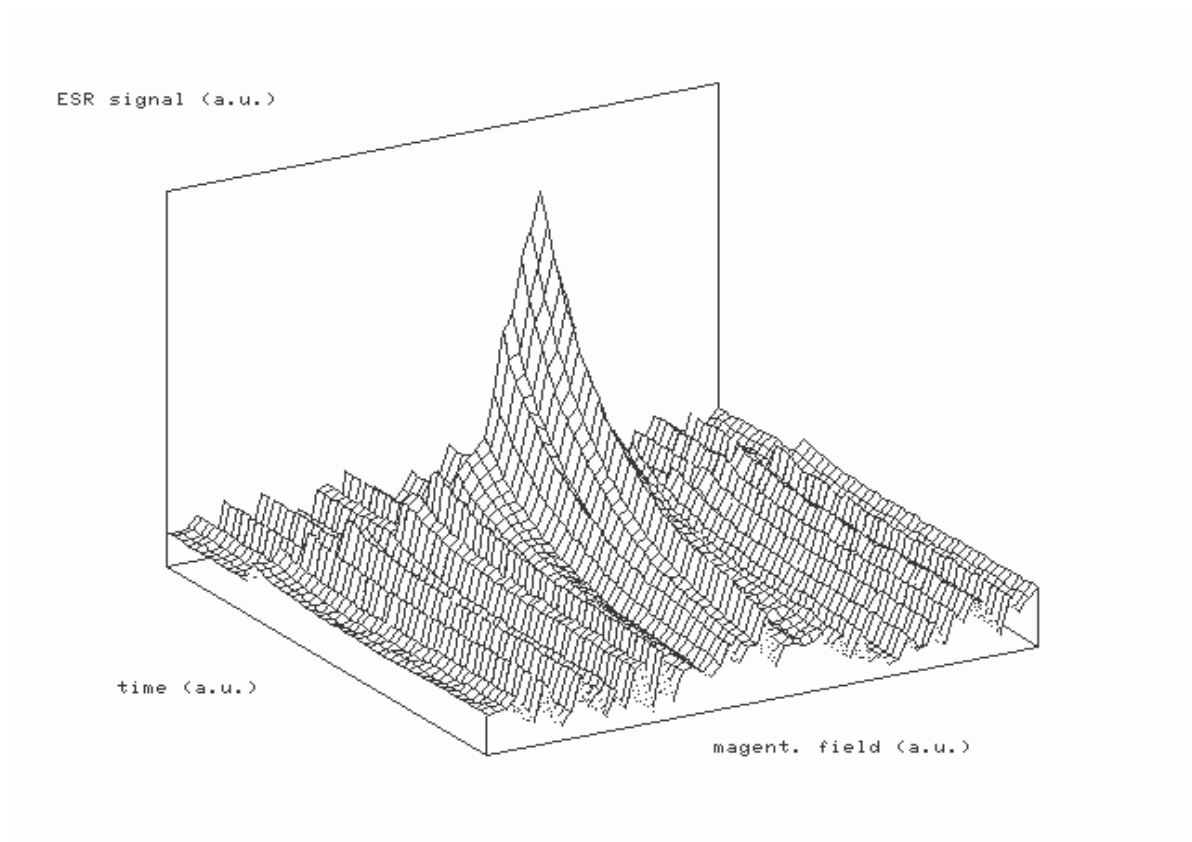
Figure 3.3: Illustration of a two-dimensional plot of the signal versus time along one axis and field along the other. The spectrum shows the time evolution of the photoexcited C_{60} in solution

Assuming that the decay rate of the excited state is small compared to the relaxation rates and $T_1 = T_2$ the on-resonance case can be described by [5]

$$A(t) = A_0 \cdot \exp(-t/T_2) \cdot \sin(\omega_1 \cdot t)$$
(3.10)

Another consequence of high microwave field strength is the appearance of side bands when reconstructing the spectrum at a certain time after the laser flash (field domain). This can lead to misassignment of some features of the spectrum. Therefore care has to be taken, to avoid strong transient nutations, when spectral information is of interest.

3.4 Limits of the Technique

3.4.1 Background signal

In addition to resonant signals from paramagnetic species, the impact of the laser beam generates at least two more signals. One originates in photo-induced release of electrons from the cavity walls and the sample (photo-effect). In general this signals last for less than 1 µs. The second unwanted effect of the input laser pulse is to cause detuning of the spectrometer as the cavity and the sample warms. This produces a slowly varying signal that is observed even off resonance and which persists typically for a few microseconds.

3.4.2 Sensitivity

Compared to ordinary electron spin resonance spectroscopy the sensitivity of TRLESR is rather low. No lock-in technique can be used and the only procedure to increase the signal to noise ratio is averaging the transients. Some of the sensitivity lost by bypassing the phase-sensitive detection can be gained back by a process called chemically induced dynamic electron polarisation (CIDEP). Due to this effect, polarisations 10-100 times the polarisation at thermal equilibrium can be observed at short times after the laser-flash. Therefore paramagnetic intermediates can sometimes be detected at even lower concentrations than stable or equilibrated species.

3.4.3 Resolution

Time-resolution of a spectrometer for TRLESR is determined either by the time constant of the detection system (bandwidth of the microwave-diode, preamplifier) or by the characteristic response-time of the resonant microwave cavity. In the first case the time resolution of the system can easily determined by

$$\tau \approx \frac{1}{bandwidth} \tag{3.11}$$

Using that a resonant cavity is the microwave analogue of a rf-tuned circuit [6], the time-resolution of the spectrometer, if limited by the cavity, is given by

$$\tau = \frac{Q}{2 \cdot \pi \cdot \nu_0}$$ (3.12)

where Q is the quality factor of the cavity and ν_0 is the microwave frequency. This shows that small Q values are required for high resolution in the time-domain, on the other hand a small Q value causes low sensitivity of the spectrometer. A response time of ~20 ns corresponds to a Q-value of 1000 at 9.5 Ghz (X-band).

3.5 Chemically Induced Dynamic Electron Polarisation (CIDEP)[7][8]

Radicals observed very soon after their creation are found normally to exhibit ESR spectra that reflect great deviations of the population from their equilibrium values. Some are observed wholly in emission, some in enhanced absorption and some combinations of the two, with some lines in emission and some in absorption. This phenomenon is commonly known as chemically induced dynamic electron polarisation (CIDEP) and also as electron spin polarisation (ESP).

The polarisation may differ for each hyperfine line in the spectrum and for a given hyperfine line it is defined as

$$P_i = \frac{(n_\alpha - n_\beta)_i}{(n_\alpha + n_\beta)_i}$$ (3.13)

where n_α and n_β are the number of electrons in the upper and lower spin state respectively.

Two basic mechanisms have been described for explaining ESP of radicals in solution: the triplet mechanism (TM) and the radical pair mechanism (RPM). A third, the correlated radical mechanism (CRM), a variant of the RPM, can be applied to systems with low radical mobility.

In the TM, radicals are created from a short-lived triplet state which is itself spin-polarised as a result of a spin-selective intersystem crossing (ISC) from the photoexcited triplet state. Electron transfer from the excited triplet state to another molecule with conservation of the electron spin alignment, within the spin-relaxation time then yields a pair of spin-polarised radicals. They are identically polarised and may exhibit spectra either in emission or in enhanced absorption dependent upon the specific levels connected in the ISC process. TM polarisation produces spectra whose lines have the relative intensities of equilibrated radicals, but their absolute intensities are changed.

When the radicals are generated from an excited singlet state, the sum of their magnetic moments must be zero to obey the law of conservation of angular momentum. Considering the whole ensemble of spins, the population of the upper spin levels must be equal to the lower ones. In other words, right after a short laser flash, no ESR signal can be observed. In the short time the two radicals remain together, they experience a strong exchange interaction, which becomes negligible small on diffusion. During the time t the radicals remain apart, the two radical spins precess around the magnetic field vector of the ESR spectrometer each at their own Lamor frequency. Therefore at a given time t' the phase difference of the spins of the two radicals and consequently their vector sum is different from zero. If the radicals now meet again and experience a non-negligible exchange interaction, this nonzero phase difference together with a certain probability of recombination during the reencounter, gives rise to a population difference of the upper and lower spin levels of the surviving radicals that may differ drastically from the equilibrium values.

In systems with no radical diffusion, the matter is even more complicated. The radicals do not move and in principle experience the exchange and dipolar interaction during their entire lifetime. The four eigenstates of the two-spin system are then no longer the pure singlet and triplet states but consist (in the high field approximation) of two (upper and lower) triplet states and two that are mixtures of the singlet and the triplet state. Depending on the precursor (singlet/triplet) the states are populated, in proportion to their spin character (singlet/triplet) and transitions between all the

different states can be induced. Again some lines may appear in absorption some in emission.

References

[1] Modern Pulsed and Continuous-Wave Electron Spin Resonance, Chapter 7, Larry Kevan and Michael K. Bowman (eds.), John Wiley & Sons, 1990

[2] C. D. Buckley, K. A. McLauchlan, Mol. Physics, 1985, Vol. 54, No.1, 1-22

[3] G. Kothe, S. Weber, R. Bittl, E. Ohmes, M. C. Thurnauer, J. Norris, Chem. Phys. Letters, Vol. 186, **6**, 474, 1991

[4] J. A. Weil, J. R. Bolton, J. E. Wertz, Electron Paramagnetic Resonance. John Wiley & Sons, 1994

[5] S. S. Kim, S. I. Weissman, Chem. Phys. Letters, Vol. 58, 3, 1978, 326

[6] Ch. P.Poole Jr., Electron Spin Resonance, Dover Publications (1983)

[7] P.J. Hore, K. A. McLauchlan, Journal of Magn. Res., 36, 129-134 (1979)

[8] The Photosynthetic Reaction Centre, Vol. II, Chapter 12, J. Deisenhofer (ed), Academic Press (1993)

Chapter 4

The Experiment

4.1 Sample Preparation

Materials under investigation were dissolved in appropriate solvents and carefully mixed to achieve certain concentrations of the components in solution. To remove the dissolved oxygen, argon was bubbled through the solutions.

All materials were used as received without any further purification. Master solutions of C_{60} (MER 99.5%+) were filtered using a 200 nm RC-filter.

Liquid samples were prepared by pouring the mixture into an ESR-tube, deoxygenating by subsequent freeze-pump-thawing cycles and sealing under vacuum.

To prepare films of polymer-fullerene composites, again the solution was poured into the ESR-tube. Evaporating the solvent using a vacuum pump, the film was formed on the inner walls of the tube. To keep the oxygen concentration low, the tube is sealed under vacuum. Care has to be taken that all the solvent is removed. Otherwise, there is no long-term stability of the film and changes in the morphology can be observed.

4.2 Components and Experimental Set-up

Coherent Infinity 40-100 Nd:YAG laser

Lambda Physics Scanmate OPPO

3M Multimode Silica Silica fiber 0.16 NA

Newport 818-BB Silicon photodiode (rise-time <150 ps, fall-time <350 ps)

Bruker EMX ESR Spectrometer

Tektronix 754C Oscilloscope (500 MHz bandwidth, 2 Gs/s, extended memory 200 Mpoints/ch)

Experimental set-up
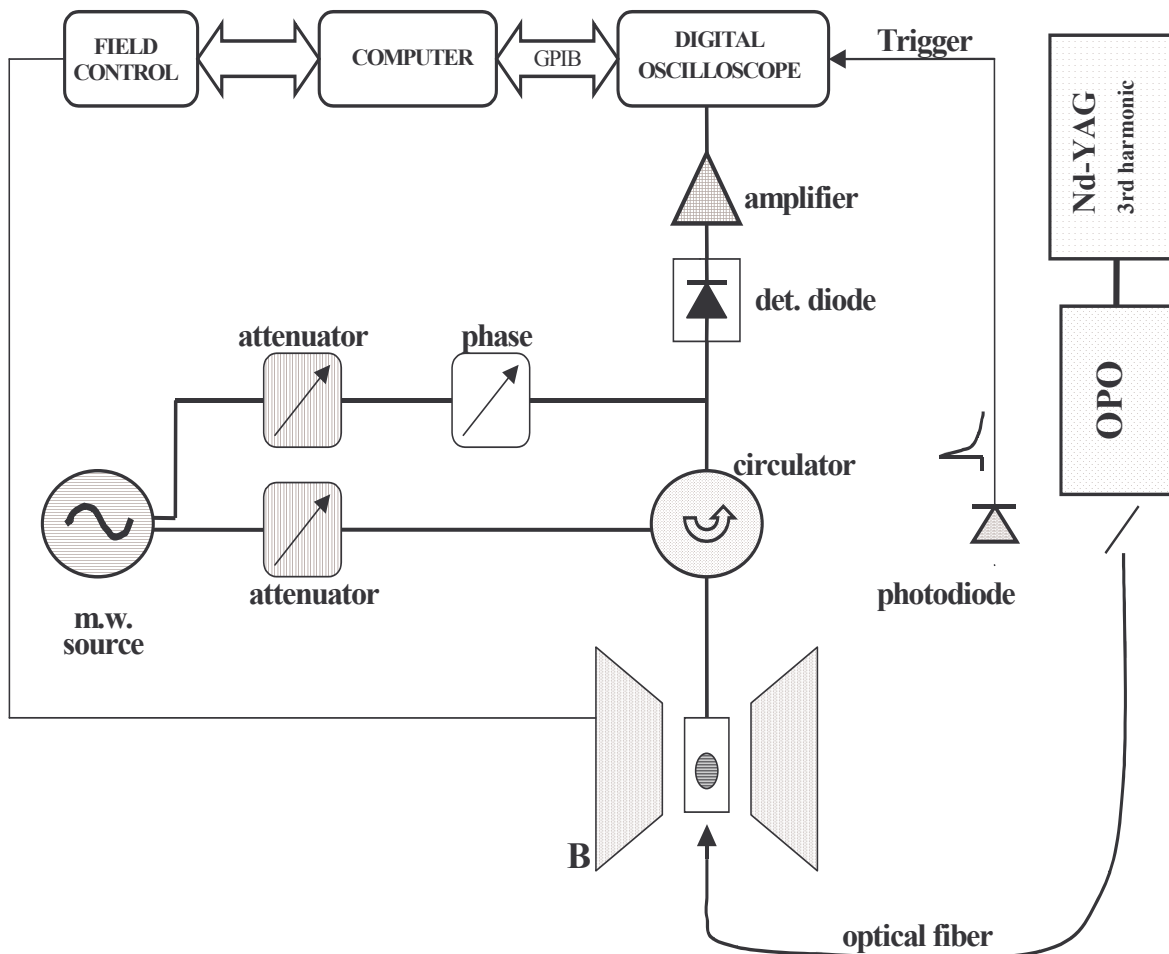
Figure 4.1: Schematic description of the TRLESR set-up

Q-switched Nd-YAG laser

The Infinity 40-100 is a diode pumped Q-switched Nd:YAG laser. It produces ~3 ns long pulses with energies up to 500 mJ at 1064 nm. One part of these pulses is frequency doubled in a non-linear optical crystal (second harmonic generation). The resulting pulse is frequency mixed with the second part of the initial pulse (again in a crystal with non-linear optical properties). In this way, the third harmonic of the pulses

of λ =1064 nm are created. In Tab. 1, some of the technical specifications of the laser

are shown [1].

Table 3 [1]: Specification of the Infinity 40-100

Wavelength	355 nm
Max. pulse energy at 355 nm	200 mJ
Pulse width at 355 nm	3 ns
Linewidth Single-longitudinal mode single shot (typical)	<2x transform limit <250 MHz

OPO (optical parametric oscillator)

The principle of the OPO can most easily be understood as the inverse of the non-linear frequency mixing process. A laser source of frequency ν_P provides the pump wave to a non-linear optical crystal. In the crystal the energy of the pump photon is transferred to two other photons (Fig. 4.2). By convention, the emitted higher-frequency photon is termed signal (ν_S) and the lower-frequency photon idler (ν_S). Signal and idler satisfy the energy conservation law

$$\nu_P = \nu_S + \nu_I \qquad (4.1)$$

and the momentum conservation law

$$\vec{K}_P = \vec{K}_S + \vec{K}_I \qquad (4.2)$$

where $\vec{K}$ is the wave-vector.

For a fixed pump wavelength these equations can be fulfilled by an infinite number of signal and idler wavelengths. However, a specific phase relation of all three waves must also be maintained within the crystal expressed as

$$n_P \cdot \nu_P = n_S \cdot \nu_S + n_I \cdot \nu_I \qquad (4.3)$$

with n_P, n_S, n_I as refractive indices at pump, signal and idler frequency respectively. The angular dependence of the birefringence in typical non-linear
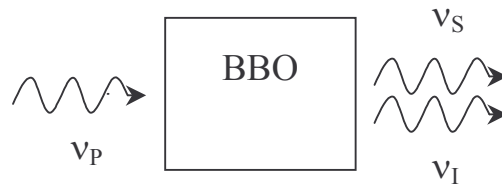
Figure 4.2: Schematic picture for the non-linear optical processes in an OPO

crystals leads to a selection of three frequencies, which meet all the conditions mentioned.

By placing the paramagnetic gain medium (non-linear crystal, BBO) in an appropriate resonator and by changing the incidence angle of the pump beam, a tuneable output between 420 nm-700 nm (signal wave) and between 710 nm-2400 nm (idler wave) can be achieved. To produce spectral narrow output pulses, the whole system consists of two different resonators (a dye-laser as a master oscillator; power oscillator BBO crystal). A schematic scheme of the SCANMATE OPPO [2] is shown in Fig. 4.3.
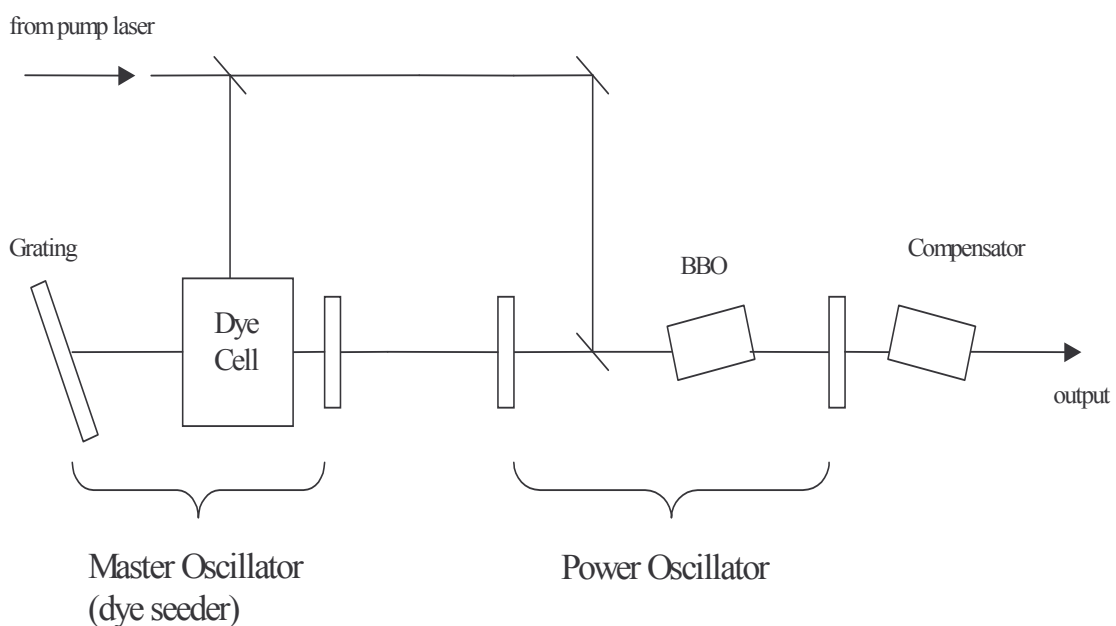
Figure 4.3: Optical scheme of the SCANMATE OPPO [2]

Via a beam splitter, a few mJ of the pump beam are coupled into the master oscillator. The resonator of this oscillator can be tuned by tilting a diffraction grating. Using different dyes, the lasing wavelength can be varied over a broad range. The output of the master oscillator serves as injection seeder for the OPO in the signal wavelength range λ_S. The injection seeded photons determine the spectral bandwidth of the power oscillator. If an unseeded power oscillator with a typical bandwidth of 10 cm^{-1} in injection seeded with a 0.2 cm^{-1} line width source, the output collapses to 0.2 cm^{-1}. Using a Q-switched Nd-YAG laser of less than 0.01 cm^{-1} bandwidth, the Scanmate OPPO in the configuration shown above has a typical line-width of 0.07 cm^{-1} [2]. Fig. 4.4 shows the importance of seeding for the output energy of the OPO. The dye used in the master oscillator is Rhodamine G6. The pulse-energy increases by a factor of 2 around the maximum emission of the dye.
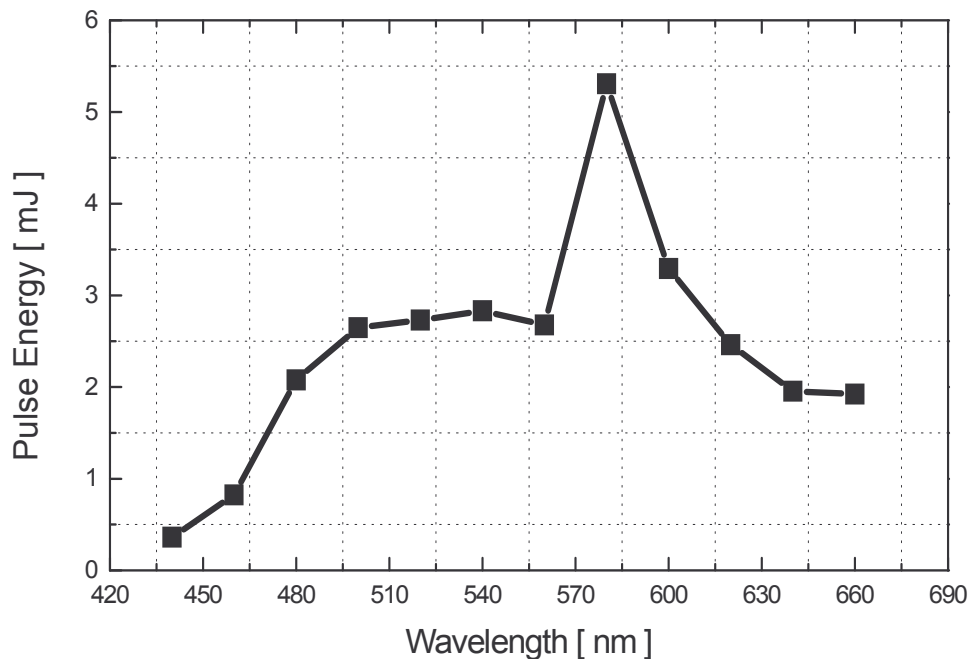
Figure 4.4: Pulse-energy vs. wavelength; the pumping energy for the OPO is kept constant (400 mJ, 1064 nm)

Optical path of the light pulses

Using a lens on a xy mount and a fiber connector on a z translation stage, the pulses

are coupled into a fiber. The fiber used is a 10 m long 3M POWER-CORE 0.16NA

Silica-Silica multimode fiber. The characteristic transmission as a function of the

wavelength and the refractive index profile are shown in Fig. 4.5 and Fig. 4.6. Other

characteristic data are given in Table 2.

Table 4: Technical data of the 3M-NA 0.16-Silica-Silica Multimode Fiber [3]

Core Diameter	Clad Diameter	Buffer Diameter	Numerical Aperture	Power Capability Pulsed[**]	Power Capability Cw
600 µm	750 µm	1250 µm	0.16	9.0 MW	1.8 KW

[**]based on 5 GW/cm^2 for 1064 nm Nd-YAG laser with 10ns pulse width and input spot size of 80% of the core diameter

Refractive
Index

Refractive Index Profile
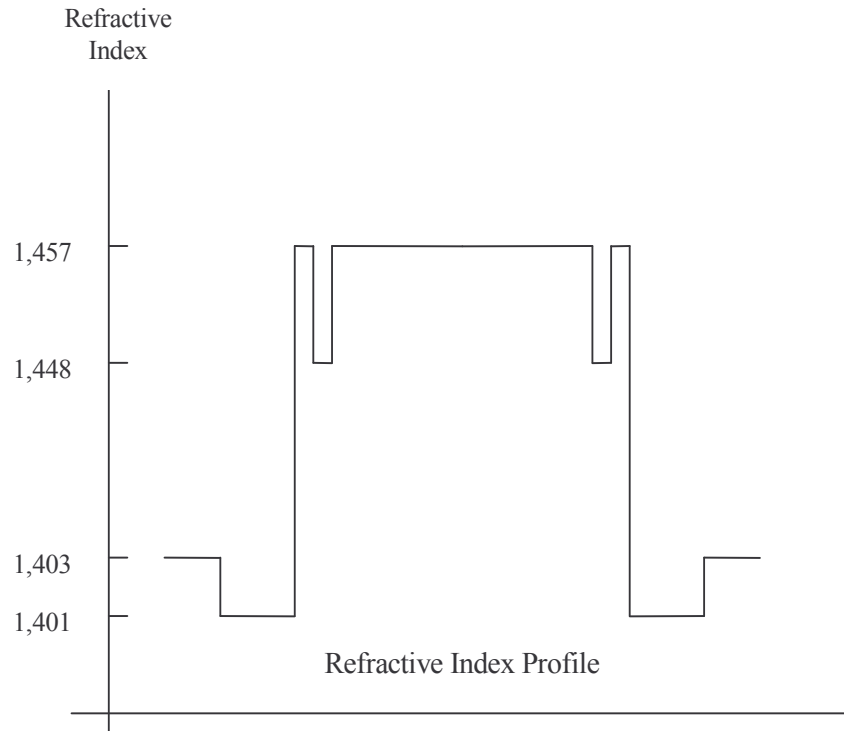
Figure 4.5: Refractive Index profile of the fiber used in the experiment [3]
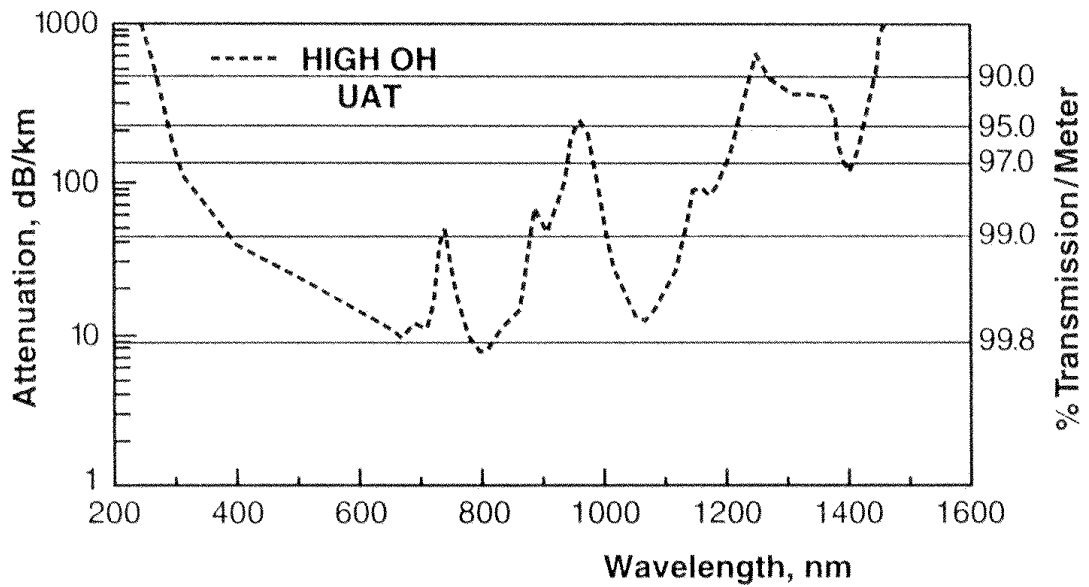
Figure 4.6: Transmission/Attenuation profile of the fiber used in the experiment [3]

To achieve good coupling, a focusing lens with

$$\frac{D}{2f} = NA \tag{4.4}$$

has to be chosen, where D is the diameter of the lens, f the focal length and NA the numerical aperture of the fiber. NA is given by

$$NA = \sin\theta_0 = \sqrt{\left(n_1^2 - n_2^2\right)} \tag{4.5}$$

where n_1 is the refracting index of the core and n_2 is the refractive index of the cladding. The focusing lens used here is AR coated (300-600 nm) with a focal length of 15.36 mm and an exit pupil of 5 mm. To avoid very high light intensities on the fiber front face, the focus has to lie between the lens and the fiber end. The dispersion of the pulse (spreading in width) as it travels along the fiber is very small. Fig. 4.7 and Fig. 4.8 show the pulse-width (FWHM) as a function of the wavelength and the pulse-energy before and after the optical fiber. The measurements were carried out
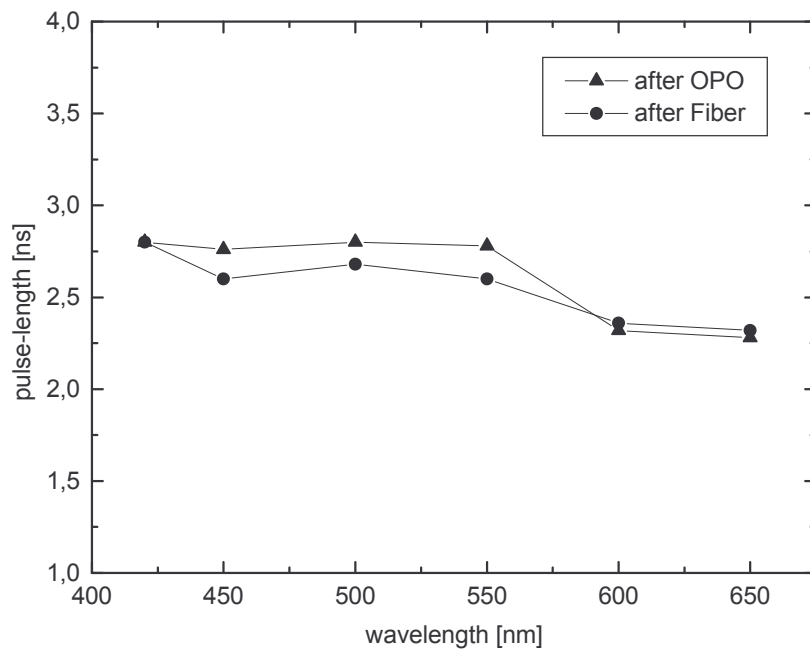
Figure 4.7: Pulse width vs. wavelength measured before and after the optical fiber
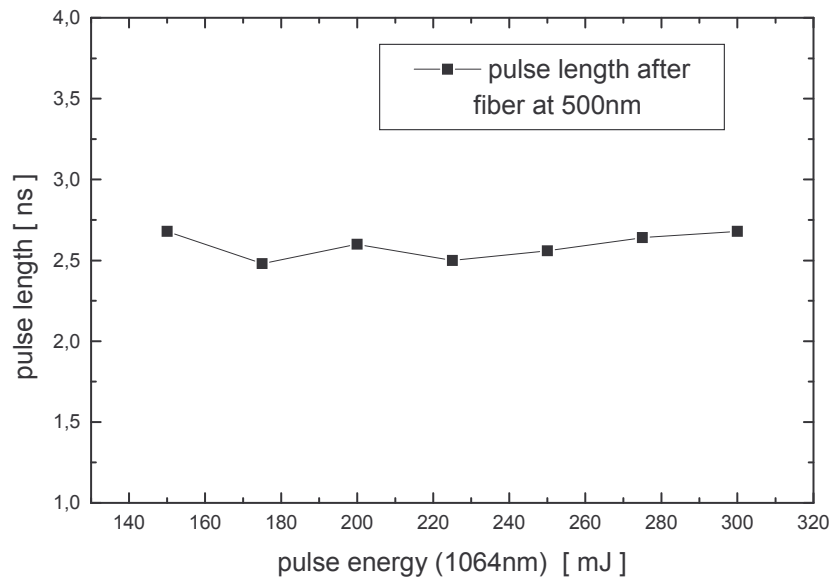
Figure 4.8: Pulse width vs. pulse energy (at λ=500 nm)

using the fast photodiode (rise-time 150 ps) and a digital storage oscilloscope. No significant changes can be observed.

Care has to be taken that the cleaved ends of the fiber have a good optical quality. Local absorption of light due to imperfections (scratches etc.) can cause serious damage to the fiber.

ESR Spectrometer

The ESR spectrometer in the set-up is a conventional spectrometer (BRUKER EMX) equipped with a special microwave bridge (ER 047 XG-T). It holds two different signal detection pathways. One, based on a microwave diode, with a fixed gain and a bandwidth of 6.5 MHz, which is also used for cw-detection and one with tuneable gain (6 dB - 72 dB) and tuneable bandwidth (25 MHZ - 200 MHz) which can be used for fast transient experiments. In the second case microwaves are detected by a wave-mixer. To stabilise the output frequency of the microwave source (gun-diode) in addition to AFC (automatic frequency control) a reference cavity can be used. The magnetic field is measured using a gaussmeter and a NMR probe.

The experiments were performed with three different cavities. One with a Q-value of ~1500 (unloaded) and an optical transmission grid for light excitation. The other two cavities have a Q-value of ~3500 (unloaded) and a transmission grid and a rectangular optical window for direct access respectively.

A liquid N_2 flow cryostat (BRUKER) and two liquid He flow cryostats (Oxford CF935, Oxford ERS 900) allow the measurements to be carried out in the temperature range between 4 K-300 K.

4.3 The Way an Experiment is performed

After aligning the optical path for the laser pulses and placing the sample in the microwave cavity, the spectrometer has to be tuned. Microwave bridge and cavity are tuned when the microwave frequency of the gun diode coincides with the resonance frequency of the loaded cavity, and the detection system is working in the linear regime.

Working with the 6.5 MHz detection system tuning the spectrometer is the same procedure then for the phase-sensitive detection measurement [4].

Broad band detection only makes sense, when the Q value of the sample cavity is small. However, the resonant mode of a low Q cavity is not very distinct and it is difficult for AFC (automatic frequency control) to lock on this mode. An additional cavity has to provide a reference signal to stabilise the gun diode output frequency and the spectrometer has to be tuned in a different way. 'BROADBAND ON' and 'STABIL ON' (bottoms on the front panel of the microwave bridge) has to be switched on when the spectrometer is in the 'Tune, dual trace' mode. Two tuning patterns appear on the screen, one for the sample cavity and one for the reference cavity. Now the wheel on the bridge front panel can be used to move the reference mode until it coincides with the sample mode (the frequencies of the two cavities are then the same). If the phase of the two modes is correct, they are locked together as soon as the spectrometer is switched to the operation mode. The further procedure is the same then above [4].

The 3 ns pulses coming from the OPO with a repetition rate of up to 50 Hz and typical pulse energy of ~1 mJ illuminate the sample.

The digital storage oscilloscope, catching the transients following each laser flash, is directly connected to the chosen amplifier. It is triggered by the fast photodiode. To achieve a better S/N ratio the transients have to be averaged. It is necessary to store not only the transient signal following the trigger, but also some of the pre-trigger signal. Using this as a baseline, the transients can be corrected for offset changes occurring during the experiment. The magnetic field is controlled by the Bruker-software. No magnetic field-modulation is used. The field can be either set manually to a certain value (Mode 1) or it can be continuously increased by a constant rate (Mode 2). Working in mode 2, the transients do not correspond to a single magnetic field value, but a small interval ΔB. The transfer of the transients from the oscilloscope to a computer is controlled by a home-made program called Getwave.tst. It is based on TestPoint[1] transferring the data via the IEEE-bus. The program creates a file holding the transients and further data to reconstruct the corresponding magnetic field values. In order to correct the spectra for non-resonant signals, caused by the laser impact, one transient is recorded out of resonance. It can be used to correct the entire resonance spectrum.

4.4 Data Acquisition

As mentioned above, the home made program Getwave.tst based on TestPoint[1] and an IEEE card is used to transfer data from the oscilloscope to the computer during the experiment. The program reads a number of parameters entered by the user (number of transients to be stored, value of the magnetic field the scan starts, scan-width, scan-time, delay between two storage procedures) and creates a file holding parameters for reconstructing the spectra in the header, and the transients. The magnetic field corresponding to each transient is acquired using the experimental time, starting at 0 at

---

[1] TestPoint is a software package for designing test, measurement and data acquisition applications (Capital Equipment Corp.)

the beginning of the experiment. The magnetic field is gradually increased by the EMX-controller and its value can be determined knowing the exact time relative to the beginning of the experiment.

After the experiments, another home made program (spectrum.cpp) reads this file, performs the baseline correction and if specified by the user the correction for the background and reconstructs the ESR-spectrum at a time after the laser pulse specified by the user. The reconstructed spectrum is stored in another file. Descriptions of the two programs can be found in Appendix A.

4.5 Light-induced ESR (LESR)

LESR is a technique to study steady state concentrations of light-induced species. The sample is illuminated by a cw-light-source and phase-sensitive detection is used to investigate the created paramagnetic particles. This technique may help to find the positions of the light-induced lines (in the magnetic field domain) also for TRLESR measurements. Therefore very often LESR experiments are carried out before starting time resolved measurements.

The light induced Electron Spin Resonance experimental procedure consists of the following steps [5]:
(1) record the ESR spectrum of the non-illuminated sample;
(2) scan the ESR spectrum under light illumination (cw)
(3) turn-off the illumination and scan the ESR spectrum again

Using this sequence of experiments the light-induced part of the spectrum can be extracted. To remove the persistent part of the signal the sample has to be warmed up to room temperature.

References:

[1] Operator's Manual, The Coherent Infinity^{TM} 40-100, Nd:YAG Laser System, Chapter 2.14

[2] Instruction Manual OPPO (10/96), Lambda Physik

[3] Thorlabs, European Catalog, 1998, 177

[4] Bruker, EMX User's Manual, Chapter 3.7

[5] V. V. Dyakonov, G. Zoriniants, M. Scharber, C. J. Brabec, R. A. J. Janssen, J. C. Hummelen, N. S. Sariciftci, Phys. Rev. B (in press)

Chapter 5

Proof of Existence

To demonstrate, that the designed set-up for the TRLESR experiment is working, reference systems were investigated. It is well known from literature, that C_{60} shows a large transient ESR signal [1]. The other system being chosen is a mixture of zinc-tetraphenylporphyrin (ZnTPP) and benzoquinone (BQ) in absolute ethanol. It is one of the most prominent exhibiting a charge transfer and dynamic spin polarisation [2].

5.1 C_{60} Triplet in Solution

In the presence of an external magnetic field intersystem crossing is highly selective in populating the three triplet sublevels (Fig. 5.1). Therefore this process can lead to spin polarisation. The photoexcited states of C_{60} exhibit analogous features to those observed in conventional π-conjugated chromophores and polymers [3]. The photoexcited triplet state of C_{60} is formed with a quantum yield of unity [3] and optical studies suggest a triplet-lifetime of 40 µs and longer [1].

The first magnetic resonance on photoexcited C_{60} was reported by Closs et al. [1] and it was assigned to the triplet state. They performed TRLESR measurements on solutions of C_{60} in toluene at room temperature and observed one narrow line (width 0.2 G) at g=2.00135. (In a more recent publication [4] a g-value of 2.0015 has been reported). The unusual narrow line-width is attributed to a very rapid interchange of the magnetic axes by pseudo rotations converting the degenerate Jahn-Teller states into each other [5].
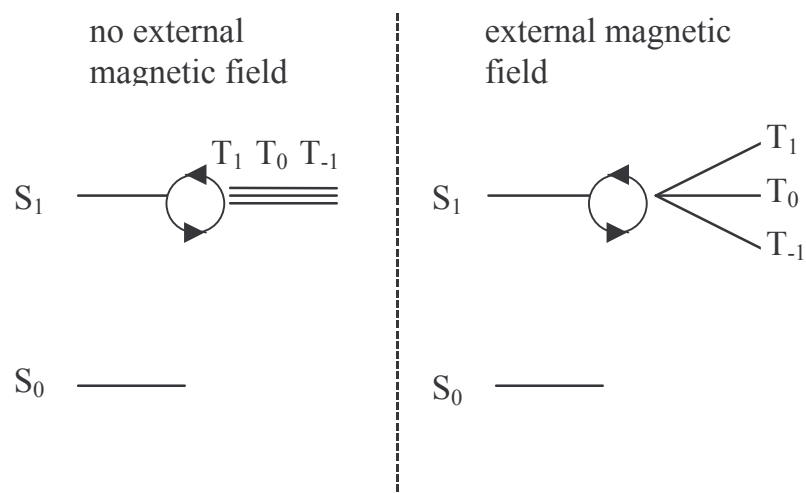
Figure 5.1: Schematic picture for intersystem crossing with and without magnetic field

In the experiments saturated solutions of C_{60} in xylene (~5.2 mg/ml) and toluene (~2.8 mg/ml) [6] were used.

The samples were placed in the grid-cavity. In order to avoid transient nutations, the microwave intensity was set to be quite small (≤6.346 mW). The measurements were

Figure 5.2: C_{60} in toluene, transient light-induced ESR spectrum reconstructed 1 μs after the laser flash (line width 0.4 G)

carried out at room temperature using the 6.5 MHz amplifier. The results of the experiment are illustrated below. In agreement with earlier results [4], one line at g=2.0015 with a line-width (lorentzian fit) of 0.4 G can be observed. The recorded line is broader than in [1] due to the higher concentration of C_{60} in the solution. In Fig. 1 the resonance spectrum 1 μs after the laser flash is reconstructed. The sample was exc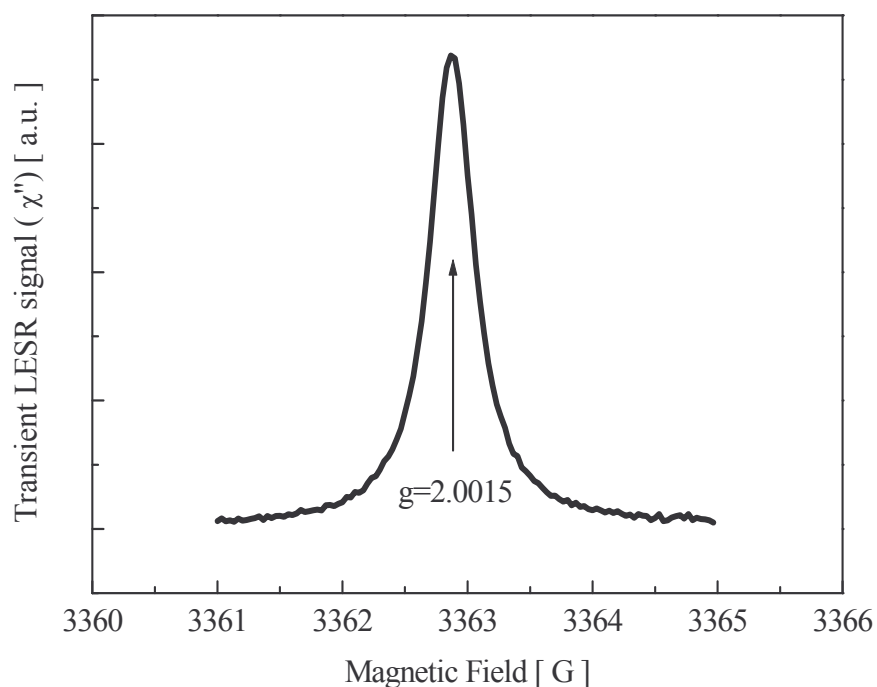ited by 1 mJ, 500 nm pulses from the OPO at a repetition rate of 31.7 Hz. In Fig. 5.3 shows TRLESR spectra of C_{60} in xylene at different times after the laser flash. 1 mJ / 523 nm pulses at a repetition rate of 27.7 Hz create the paramagnetic particles. A dynamic change of the line width can be observed. Although intersystem crossing is very fast, it takes some time for the microwave radiation to convert the initially created M_z magnetisation into detectable M_y magnetisation. Due to molecular tumbling the conversion is not a coherent process and the maximum signal intensity is reached around 1 μs after the triplet creation.
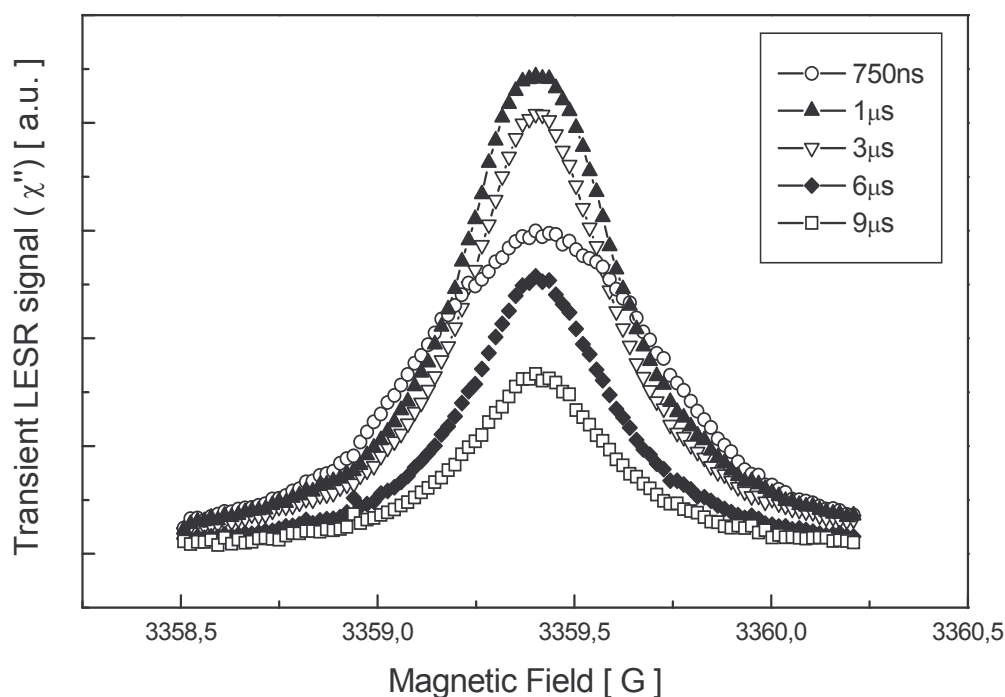
Figure 5.3: C_{60} in xylene, resonant spectrum is reconstructed at different times after the laser flash (line width after 1 μs, 0.44 G)

5.2 Transient Nutations

Setting the magnetic field to the value, which corresponds to resonance, transient nutation can occur at high microwave fields. According to theory, the maximum frequency of the additional oscillations should be microwave power input dependent. The higher the intensity of the microwave fields the higher the frequency of the oscillations. In Fig. 4 transient nutations of the C_{60}-triplet in toluene are shown. 1 mJ / 523 nm pulses excited the sample and signals were captured using the broadband amplifier.
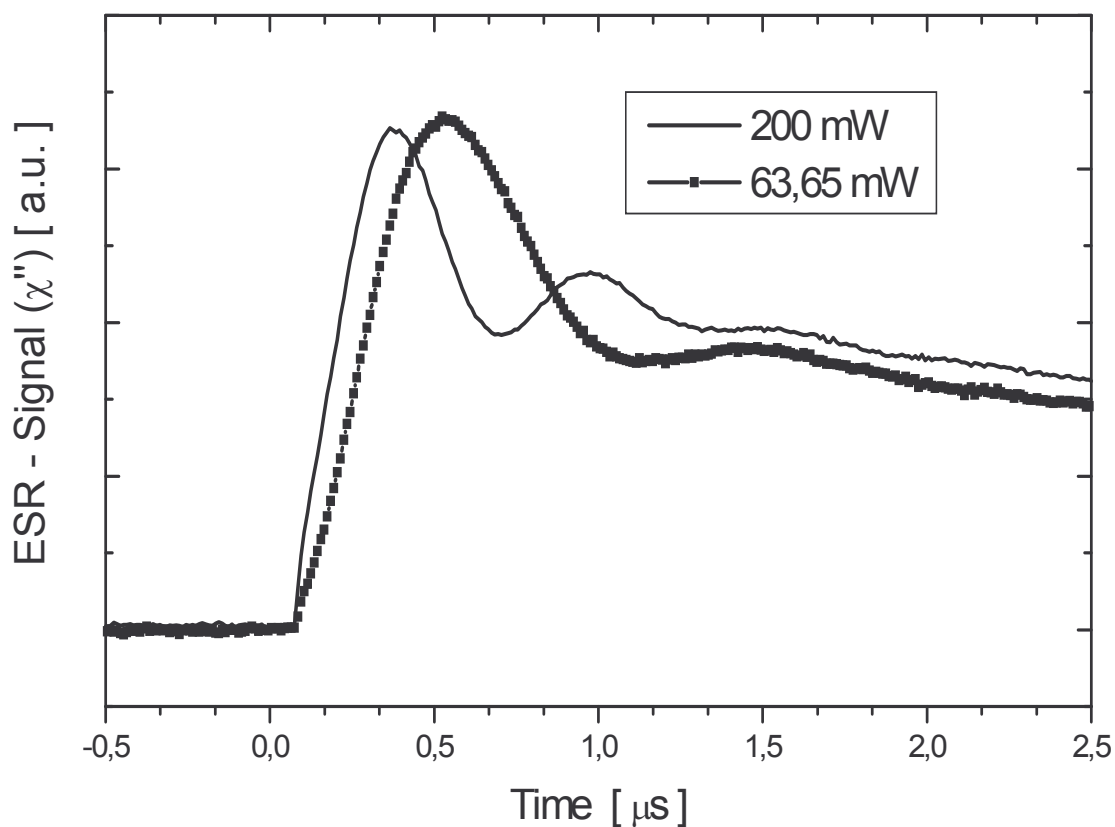
Figure 5.4: Transient nutation of the C_{60}/toluene at different microwave intensities
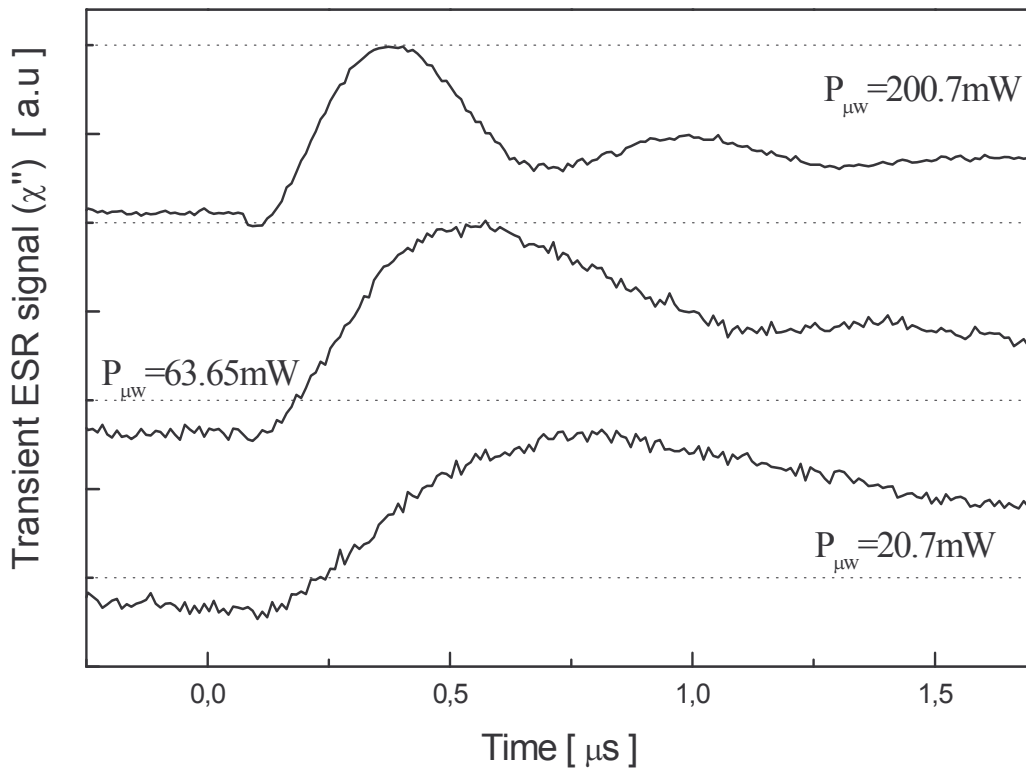
Figure 5.5: Transient nutation of the C_{60}/xylene at different microwave intensities

In Fig. 5.5 again transient nutations of the C_{60}-triplet are shown. The signals are now taken from the 6.5 MHz amplifier. Using equation (3.10) the coefficient ω_1 can be estimated and compared with the incoming H_1 for different microwave powers. For 200 mW microwave power $\omega_1(200\ mW) = 1 \cdot 10^7$ rad/s and for 63.65 mW a $\omega_1(63.65\ mW) = 5.4 \cdot 10^6$ rad/s is found. If the Q-value of the cavity stays the same for the two measurements one should find

$$\frac{\sqrt{(200\ mW)}}{\sqrt{(63.65\ mW)}} = \frac{\omega_1(200\ mW)}{\omega_1(63.65\ mw)} \tag{5.1}$$

which holds for the estimated values within the experimental error. Using again equation (3.10) also the relaxation times T_1 and T_2 can be roughly estimated. A value of ~10 µs is obtained, which is in the range of other experimental results [1].

5.3 Zinc tetraphenylporphyrin - Benzoquinone

Investigated materials
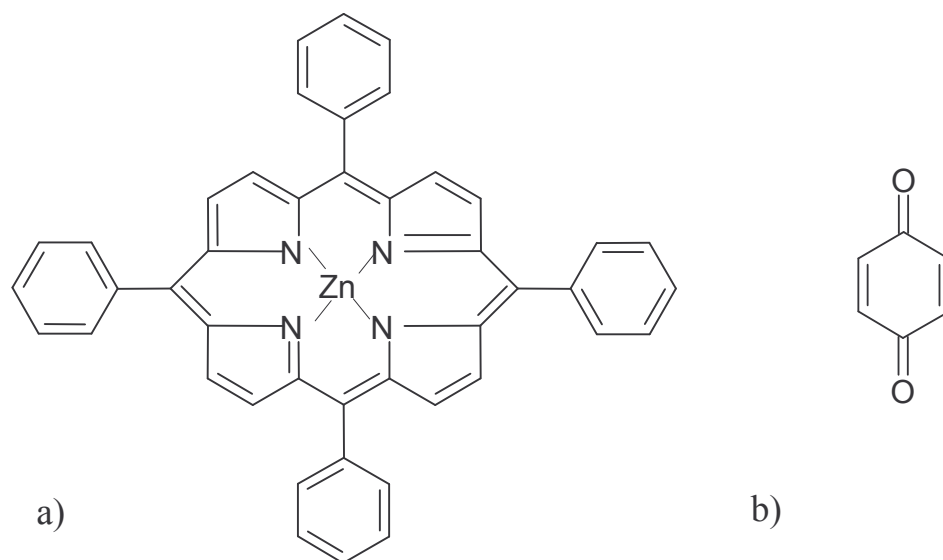
Figure 5.6: a) zinc tetraphenylporphyrin; b) benzoquinone

The reversible electron transfer from ZnTPP to BQ has been subject of numerous spectroscopic studies [2]. ZnTPP/BQ is a simple model system for photosynthesis in which porphyrins and quinones play an important role.

ZnTPP and BQ were used as received from Aldrich. Samples were prepared from a mixture of $5 \cdot 10^{-4}$ M ZnTPP / 10^{-2} M BQ in absolute ethanol. Fig. 5.7 shows the light induced ESR spectrum obtained by exciting the sample with an Ar+ laser (488 nm, P_{light}=150 mW, 100 scans, P_{mw}=2,52 mW, Modulation Amplitude 0.2 G_{pp}) using phase-sensitive detection. Five narrow lines (width 0.2 G) appear due to BQ⁻. The electron interacts with the four protons on the BQ. The relative line intensity is 1:4:6:4:1 as expected in steady state conditions. In the spectrum a hyperfine splitting constant of a_H=2.36 G can be observed. The spectrum does not show the ZnTPP cation, which must be generated if the anion results from the photoinduced electron transfer reaction. The presence of long-lived BQ⁻ and absence of ESR evidence for the formation of the cation has been explained by side reactions in which fractions of ZnTPP⁺ are reduced by hydroquinone [7][8]. The ESR spectrum of ZnTPP⁺ would be

expected to be very broad due to the various hyperfine interactions occurring on the molecule.

Results from investigating the system using TRLESR technique are shown in Fig. 5.8 (Mode 1). Setting the magnetic field values to the positions corresponding to the maximum absorption in the LESR spectrum and to values between the lines, transient LESR
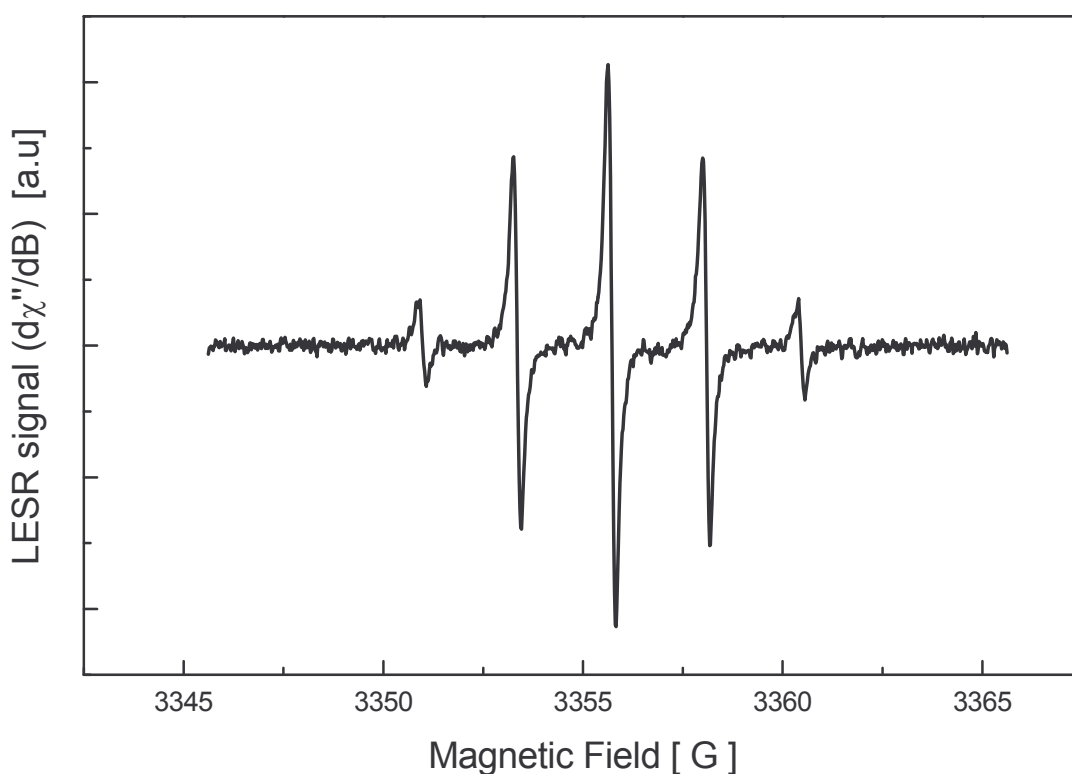
Figure 5.7: LESR spectrum of radicals generated by irradiation of a solution of ZnTPP/BQ mixture in absolute ethanol

signals were recorded. Only single points of the transients are plotted with respect to the magnetic field. Each represents the signal intensity at a certain time after the laser flash. Pulses from the OPO induced the charge transfer (λ=580 nm, pulse energy 1 mJ, repetition rate 27.1 Hz; microwave power 0.63 mW). In Fig. 5.9 the whole spectrum is reconstructed (Mode 2) at a time 1 μs after the
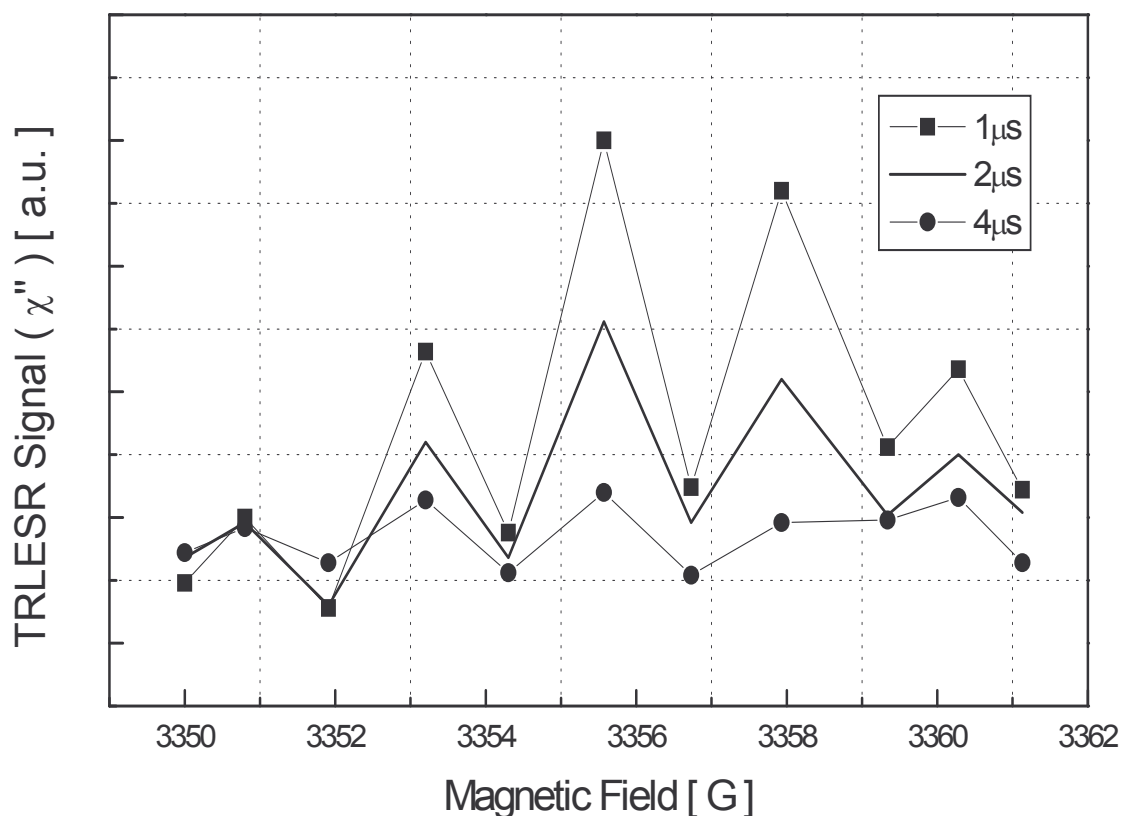
Figure 5.8: A few points of the TRLESR spectrum of ZnTPP/BQ in ethanol at different times after the laser flash

laser flash (λ=580 nm, pulse energy 1 mJ, repetition rate 27.1 Hz; microwave power 0.63 mW). The time resolved spectra show spin polarisation effects. This means, the spectra deviate from the binomial intensity distribution found in LESR. The hyperfine splitting constant extracted from Fig. 5.9 is again 2.36 G, however the relative line intensity is approximately 1:5:10:7:3.

The electron polarisation (CIDEP) is caused by the interaction of the radical pairs after the charge transfer and the triplet formation on the excited ZnTPP. The whole spectrum is sitting on a very broad background, which is attributed to ZnTPP$^+$ radical [2].
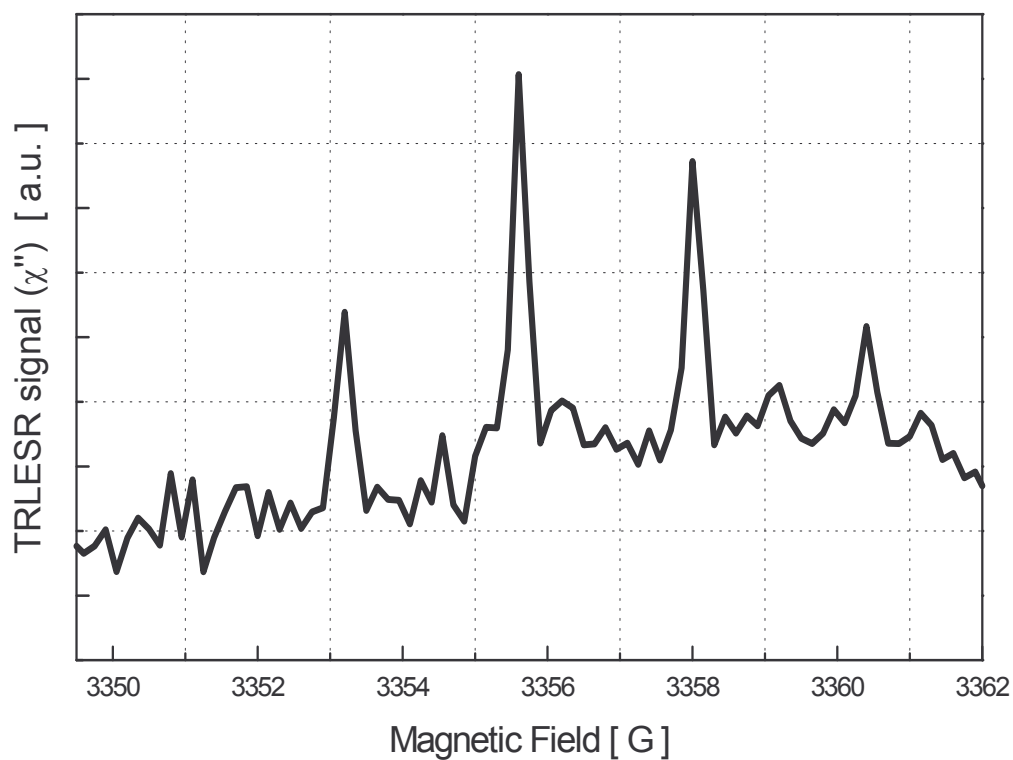
Figure 5.9: Time resolved light induced ESR spectrum of photochemically generated free radicals in ZnTPP/BQ in ethanol reconstructed 1µs after the laser flash

The presented data on the C_{60}-triplet and ZnTPP/BQ are in good agreement with results taken from the literature [1][2]. The experiments demonstrate that set-up is working.

References:

[1] G. L. Closs, P. Gantam, D. Zhang, P. L. Krusic, S. A. Hill, E. Wasserman, J. Phys. Chem. 1992, 96, 5228-5231

[2] H. v. Willigen, M. Vuolle, K. P. Dinse, J. Phys. Chem., 1989, 93, 2441-2444

[3] A. Regev, D. Gamliel, V. Meiklyar, S. Michaeli, H. Levanon, J. Phys. Chem., 1993, 97, 3671-3679

[4] C. A. Steren, H. v. Willigen, K. P. Dinse, J. Phys. Chem. 1994, 98, 7464-7469

[5] M. Bennati, A. Grupp, M. Mehring, J. Chem. Phys., 102(24), 22 June 1995, 9457

[6] R. S. Ruoff, D. S. Tse, R. Malhotra, D. C. Lorents, J. Phys. Chem., 1993, 97, 3379-3383

[7] A. Harriman, G. Porter, N. Searle, J. Chem. Soc., Faraday Trans. 2, 1979, 275, 1515

[8] B. J. Hales, J. R. Bolton, J. Am. Chem. Soc. 1972, 94, 3314

Chapter 6

Investigation of Conjugated Polymer-Fullerene Composites

6.1 P3OT - C$_{60}$ in Solution[1]

The experiments were performed on poly-3-octyl-thiophene (the chemical structure of P3OT is shown in Fig. 2.1) C$_{60}$ mixtures (0,5 mg/ml / $5 \cdot 10^{-4}$ M) and the polymer (0.5mg/ml) and the fullerene ($5 \cdot 10^{-4}$M) alone in xylene and ortho-dichlorbenzene (ODCB). The mixtures were investigated by LESR and TRLESR technique.

6.1.1 Results and Discussion

No light induced ESR-signal could be detected in P3OT in xylene. It is known from PIA (photo-induced absorption) studies that conjugated polymers undergo efficient intersystem crossing to the triplet manifold [2]. Due to the random orientation of the polymer in the solution no polymer triplet can be detected by ESR technique. The main relaxation route for the excited polymer is (S$_1$)→(S$_0$) (luminescence). Also intersystem crossing (S$_1$)→(T$_1$) occurs, but with much lower intensities.

In P3OT in ODCB we observed one very weak LESR line (g≈2.0026) which is attributed to the polaron on the polymer chain. This result is also supported by PIA studies [2] and indicates that the polarity of the solvent plays an important role. The charge transfer can either be of intrachain character or into the solvent.

As already explained in chapter 5 the dominant photoinduced signal in C$_{60}$ is the triplet.

The light induced signal recorded in a mixture P3OT - C$_{60}$ is assigned to the C$_{60}$ triplet state (g=2.0015, line width 0.3 G). No polaron and no C$_{60}^-$ can be observed. From PIA studies [2] it is known that adding C$_{60}$ to P3AT (poly-3-alkyl-thiophene) quenches the

photoexcited polymer triplet. It is suggested that energy-transfer from the polymer to the fullerene is responsible for this effect ($P3AT(T_1)+C_{60}(S_0)\rightarrow P3AT(S_0)+C_{60}(T_1)$). One would therefore expect that the fullerene triplet decay rate should change in the presence of the conjugated polymer. In the experiment the P3OT triplet is not accessible. However, one can compare the decay characteristics of $^3C_{60}$. Fig. 6.2 shows the time evolution of the photoexcited fullerene triplet states with and without polymer.
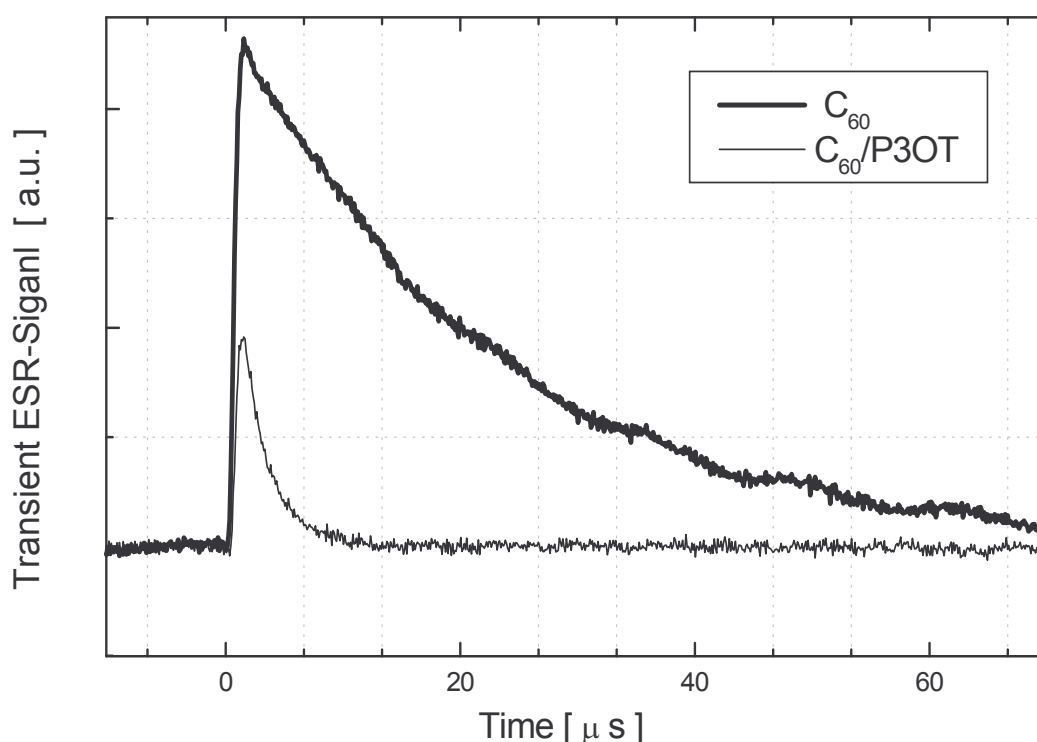
Figure 6.1: Transients taken on maximum resonance of C_{60} and C_{60}/P3OT in xylene

Also the photoexcited response of P3OT/C_{60} in ODCB was investigated by ESR measurements. Although ODCB supports charge transfer due to its high polarity no light induced ESR signal of C_{60}^- has been observed. At a g-value of g=2.0015 a weak photoinduced signal can be detected. This is again interpreted as the $^3C_{60}$ signal.

6.2 Conjugagted Polymer Fullerene Films

A detailed study on the photoinduced spins in conjugated polymer fullerene films has been carried out at our laboratory using LESR technique [3]. The findings of this study are summarised in Fig. 6.2.
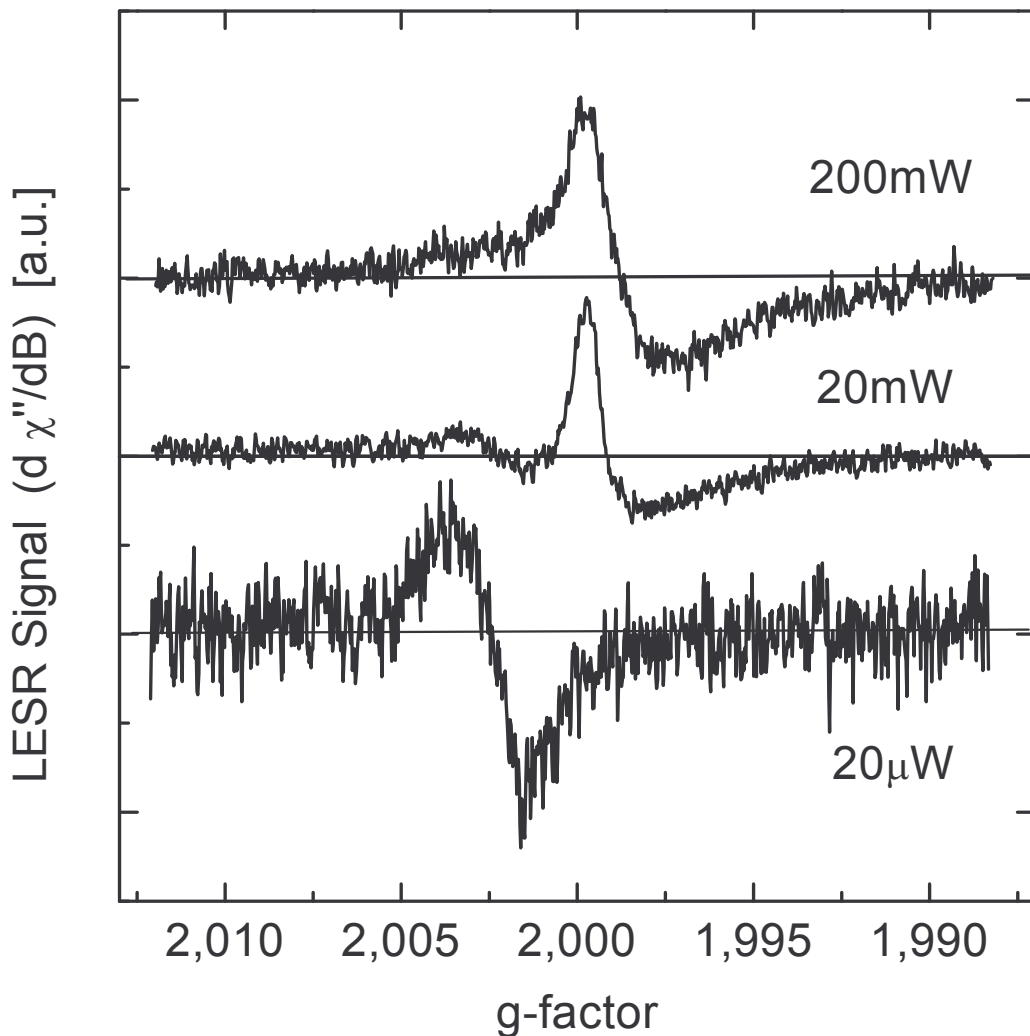
Figure 6.2: LESR spectra of MDMO-PPV/Fullerene composites at different values of microwave power. T=100 K, λ_{exc}=488 nm, P_{exc}=20 mW/cm^2 [3]

- Light induced charge transfer from the polymer onto the fullerene in the composite results in the appearance of two LESR signals. The two lines are attributed to the positive polaron on the conjugated polymer backbone (g=2.0025 for MDMO-PPV (chemical structure see Fig. 2.1)) and to the fullerene anions (g=1.9995).

- Microwave saturation studies demonstrate that the relaxation times are different for the two paramagnetic particles (Fig. 6.3).
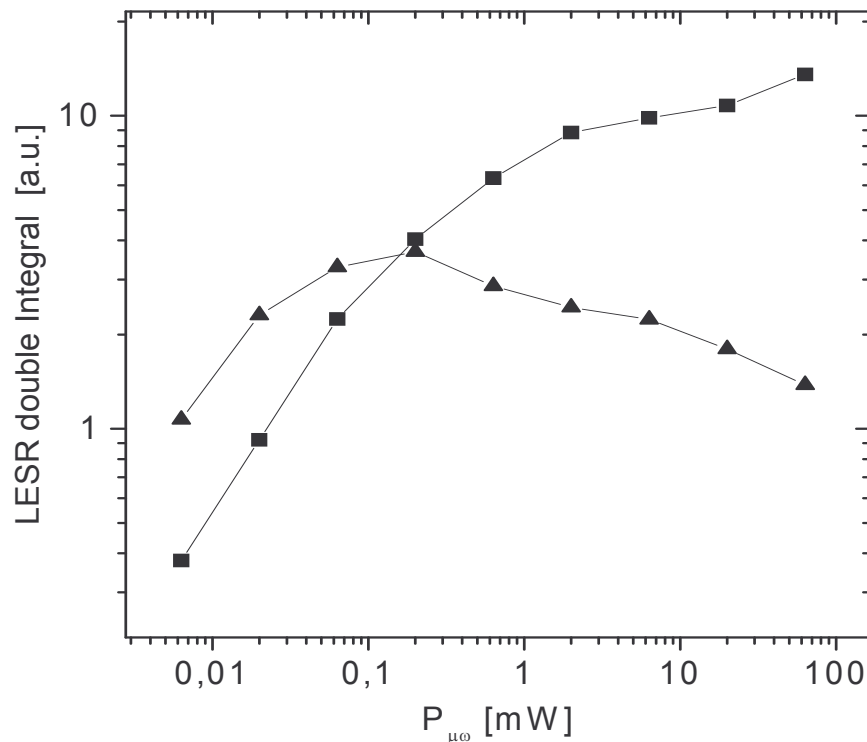
Figure 6.3: Microwave power dependence of the two observed LESR signals (double integral) in MDMO-PPV/PCBM. T=90 K, P_{exc}=20 mW/cm^2, λ_{exc}=488 nm. Squares are for the PCBM LESR line, triangles are for the MDMO-PPV LESR line [3].

- One can distinguish between a fast decaying, reversible contribution into P^+ and C_{60}^- LESR signal (prompt), and a slowly decaying (persistent) one. The prompt signal can be attributed to a bimolecular type recombination, whereas the persistent part originates from deep trap defects.

In further experiments PPV/PCBM films were investigated by TRLESR. Although the two distinct lines can be observed in LESR, no magnetic field dependent microwave absorption can be found with the TRLESR technique (Fig. 6.3). The experiment was performed at T=100 K, the sample was excited by 0.2 mJ / 500 nm pulses.
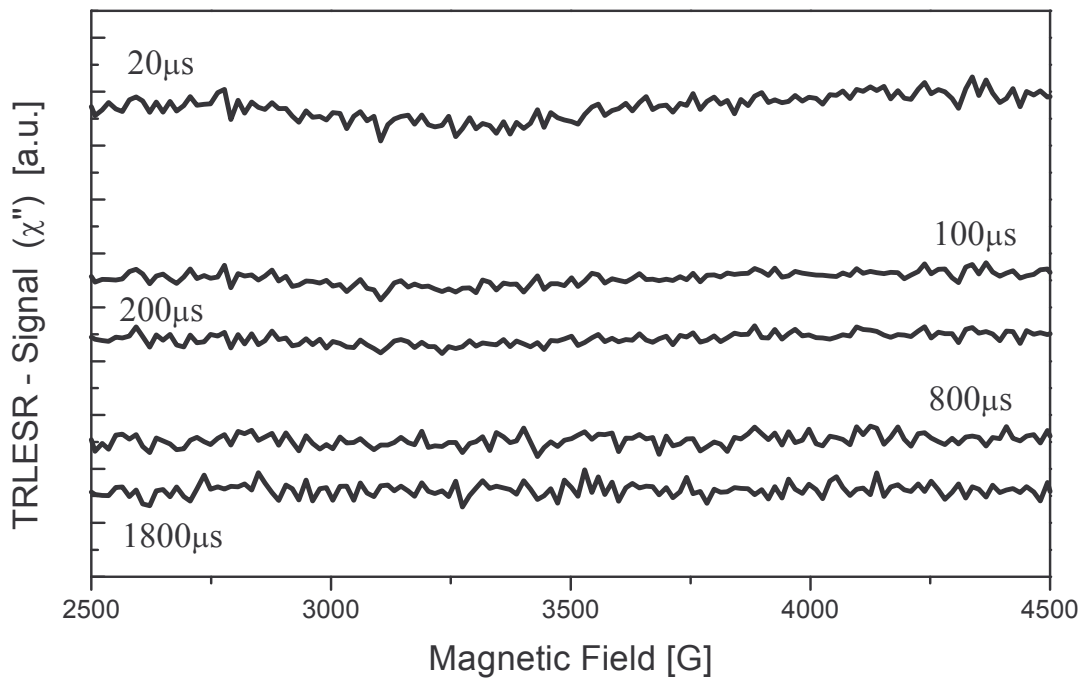
Figure 6.4: Reconstruction of the TRLESR spectrum of MDMO-PPV/PCBM

Microwave absorption of the sample following each laser flash can be observed (even at room temperature), however this occurs independently from the magnetic field. The

Figure 6.5: One single transient taken at 3340G

origin of these magnetic field independent transients (Fig. 6.3) is still not clear. It might result from thermal heating of the sample, which detunes the cavity and causes

additionally reflected microwave power from the cavity. The cavity goes only slowly back to resonance and the observed effect can be misinterpreted as transient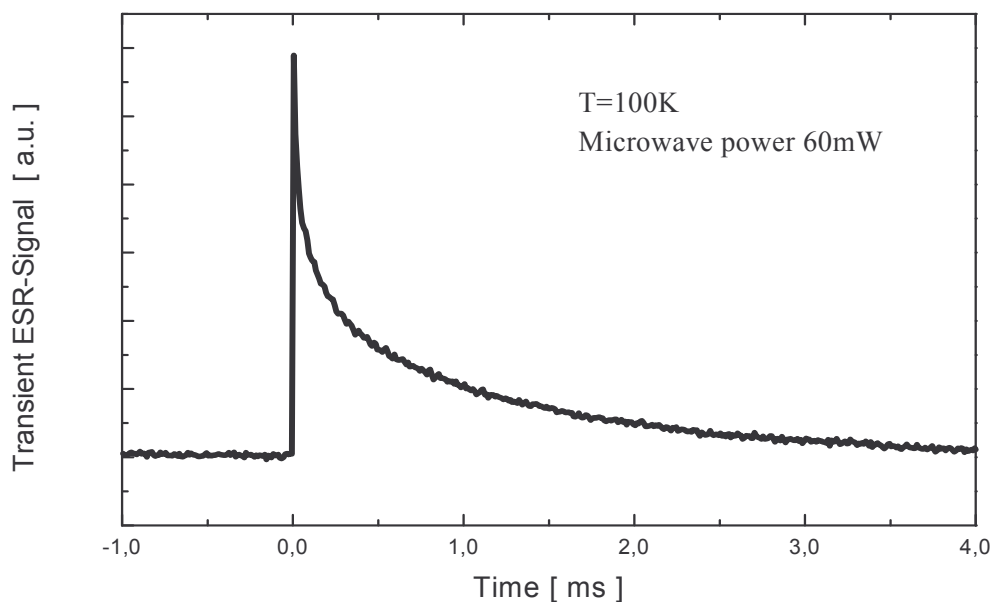 microwave absorption induced by short light pulse. Also the light induced free charge carriers in the film (photoconductivity) can cause such transient microwave absorption. The signal should again be magnetic field independent and the duration of the transient should be directly related to the lifetime of the free carriers.

Although the origin of the background is unknown, there has to be a magnetic field dependent part in the TRLESR experiments corresponding to the two lines observed in LESR, but for the investigated samples it seemed to be too small to be observed. As mentioned in chapter 3 the sensitivity of the time-resolved ESR technique is smaller than ESR based on phase-sensitive detection. And it is known from the literature that without dynamic spin polarisation effects it is very difficult to perform TRLESR experiments although a LESR signal can be easily detected for the same sample [4]. Therefore one may conclude that no radical pair or triplet mechanism is involved in the charge transfer process and therefore the effective polarisation occurring after the laser flash is below the detection limit of the spectrometer. To get higher population differences between the different spin states one can decrease the temperature. However at very low temperatures almost no light induced ESR signal can be observed. After exposing the sample to light once at temperatures ≤ 10 K no additional light induced signal can be observed when the sample is illuminated again. Therefore our experiments at very low temperatures also did not show any magnetic field dependent transient signals.

References:

[1] M. C. Scharber, C. J. Brabec, V. Dyakonov, N. S. Sariciftci, Conference Proceedings ICSM 1998, submitted
[2] Rene Jannsen, N. S. Sariciftci, A. Heeger, J. Chem. Phys. 100(12), 1994, 8641
[3] V. Dyakonov, G. Zoriniants, M. Scharber, C.J. Brabec, R.A.J. Janssen, J.C. Hummelen and N. S. Sariciftci, Phys. Rev. B, in press
[4] L. Pasimeni, M. Ruzzi, M. Prato, T. Da Ros, G. Barbarella, M. Zambianchi, Conference Proc., Electrooptical Properties of Polymers and Related Phenomena, Varenna (Italy), September 13-17, O10, 1998

Chapter 7

7.1 Summary

Test-measurements on C_{60} in solution and zinc-tetraphenylporphyrin/benzoquinon in ethanol demonstrate that the system is working.

Investigations of P3OT/C_{60} in solution show that the light induced C_{60} triplet is quenched by the presence of the conjugated polymer in solution.

Although light induced electron transfer from MDMO-PPV to PCBM can be observed with phase-sensitive ESR, this signal could not be found for the same sample in TRLESR experiments. Instead a magnetic field independent signal showed up, its origin is unknown.

7.2 Acknowledgements

8 Appendix

8.1 Getwave.tst:

The program is based on TestPoint a developing tool for data acquisition problems. It reads data captured by the Tektronix 754C oscilloscope via the IEEE bus. Before starting acquisition the user has to specify different experimental parameters:

Sets: Number of transients that should be recorded;
B-start: Starting value of the scan (magnetic field);
ΔB-width: Width of the scan (magnetic field)**:**
B-time: Time required for the scan. The Bruker Software controlling the magnetic field calculates this value. The scan time can be used to calculate the magnetic field values for the different transients.
Delay: determines the number of averages for one transient. The entered Delay times repetition rate of the light excitation is equal to the number of averages.

The program creates a file holding calibration values for the oscilloscope followed by the data for the transients plus the time the transients are recorded.

8.2 Spectrum.cpp:

This C-program reads the file created by Getwave.tst, performs the baseline correction using the pre-trigger part of the transients and if specified the correction for the background signal. After the user has specified the time at which the ESR-spectrum should be reconstructed (relative to the trigger signal) a file is created holding two columns. In the first the magnetic field values and in the second the ESR-signal-intensity can be found. A listing of the program Spectrum.cpp is printed below.

```c
#include <stdio.h>
#include <conio.h>
#include <string.h>
#include <stdlib.h>


/*********************************************************/
/* For OSZI 754C,und Testpointprogr. Getwave.tst         */
/* Other Tektronoix Oszilloskoces may produce different  */
/* Data Structures and therefore the program might not   */
/* work properly                                         */
/*********************************************************/

/* prototype */
float converttime(int, int, int);
void offset(float[5000], int, float);

main()
{

/* Declarations */

int i,j,k,l,m,dummy,pos,position,points;
float HH,MM,SS,Bstart, Bwidth, Btime;
float t0,t1;
float intro[30],intro1[30],timepkt,trigpos,timepos;
float number,vector[5000],reference[5000],B[1000];
float reconstruct[1000],delay;
char filename[30];
char filename1[30];
char *answer1 ="N", *answer2="n", *answer3="y", *answer4="Y";
char ref[30],cont[30];
FILE *fptr, *fileptr, *outptr;


/* LOOP */

do
{
 clrscr();

 /* Assigning */

 j=0;
 l=0;
 dummy=0;
 position=0;

/******************/
/* Read Reference */
/******************/

 printf("\n\nDid you record a Referenz-Spectrum?\n");
 printf("If YES enter the Filename / else enter N : ");

 scanf("%s",ref);

 if ((strcmp(ref,answer1)==0)||(strcmp(ref,answer2)==0))
   {
    dummy=0;
    printf("\nThe program will not use a reference spectrum");
    printf("\nPress any key to continue");
    getch();
   }
 else
```

```c
   {
/*****************************************************/
/* Reading FILE consisting of one Set as a Reference */
/*****************************************************/

   if ((fptr=fopen(ref,"r")) == NULL )
    {
     printf("\nFile could not be opended");
     getch();
    }

   else
    {
     printf("\nTry to read reference !!");
     dummy=1;

/* read header */

     for(i=1;i<=7;++i)
       {
        fscanf(fptr,"%f", &number);
        intro1[i]=number;
       }

/* read time information */
     fscanf(fptr,"%f:%f:%f\n",&HH,&MM,&SS);

/* read data set */

     fscanf(fptr,"%f", &number);

     while(!feof(fptr))
       {
       if (!feof(fptr))
          {
           ++l;
           reference[l]=number;
          }
        fscanf(fptr,"%f",&number);
       }
     fclose(fptr);
    }
  }


/******************************************************/
/* Read Sets to be processed; Data-Structure determined */
/* by the Testpoint Program                           */
/******************************************************/

printf("\nEnter Name of File to be processed : ");
scanf("%s",filename);


if ((fileptr=fopen(filename,"r")) == NULL )
  {
   printf("\nFile could not be opended !!");
   getch();
  }

else
  {

/* Read Header for  configuration*/
```

```
  for(i=1;i<=7;++i)
   {
    fscanf(fileptr,"%f", &number);
    intro[i]=number;
   }
/*********************************************/
/* Characteristic Parameters of the Spectrum */
/*********************************************/

  points=int(intro[3]);
  trigpos=intro[1];
  timepkt=(intro[2]/50.0);
  Bstart=intro[4];
  Bwidth=intro[5];
  Btime=intro[6];
  delay=intro[7];


/* Not correct REF.-FILE */

  if ((points!=l)&&(dummy==1))
   {
    printf("Reference and Spectrum are not consistent\n");
    printf("Processing will be without Ref.-File\n");
    dummy=0;
    getch();
   }

/* if Ref.-File ex. and correct, correct it for offset */

  if (dummy==1)
   {
    offset(reference,points,trigpos);
   }


/* Read Basic Information for the Spectrum Reconstruction */

 do
 {
  printf("Enter       the       postion       (%d       -       %d)       :
",int(points*trigpos/100.0),points);
  scanf("%d",&pos);
 }
 while((pos<(points*trigpos/100.0))||(pos>points));


 /* Calculate Time-Position (approx.) */

 timepos=(pos-points*(trigpos/100.0))*timepkt;

 printf("\nTime corresponds to T= %e  after the Laser-Flash",timepos);
 printf("\nEnter Filename for reconstructed Spectrum : ");
 scanf("%s",filename1);


/******************/
/* Read set by set */
/******************/


  fscanf(fileptr,"%f:%f:%f\n",&HH,&MM,&SS);
  t0=converttime(HH,MM,SS);
  t1=t0;
```

```
  fscanf(fileptr,"%f", &number);

 while(!feof(fileptr))
  {
   if (!feof(fileptr))
    {
     ++j;
     vector[j]=number;

     if (j==points)
      {
     ++position;
     j=0;
     offset(vector,points,trigpos);

/* Referenz Correction */

     if (dummy == 1)
       {
        for(m=1;m<=points;++m)
          vector[m]=vector[m]-reference[m];
       }


/***********************************************/
/* Read out chosen values and write it to file */
/* and determine the Field - Position using    */
/* parameters entered by the user           .*/
/***********************************************/

     /* Magnetic Field */
     B[position]=Bstart+(Bwidth/Btime)*(t1-t0+delay/2.0);

     /* Amplitude */
     reconstruct[position]=vector[pos];
     fscanf(fileptr,"%f:%f:%f\n",&HH,&MM,&SS);
     t1=converttime(HH,MM,SS);

      }
     }
    if (!feof(fileptr))
     fscanf(fileptr,"%f", &number);
   }

 }

fclose(fileptr);

/**********************************/
/* Write created Data-File on Disk */
/**********************************/


if ((outptr = fopen(filename1,"w"))==NULL)
{
 printf("\nFile could not be opened\n");
 getch();
}
else
 {
   fprintf(outptr,"%f;%f\n",timepos,timepos);
   for(i=1;i<=position;++i)
   fprintf(outptr,"%f;%f\n",B[i],reconstruct[i]);
 }
fclose(outptr);
```

```c
printf("\nDo you want to process another File?");
printf("\nEnter y for yes any other key to cancle the program:    ");
scanf("%s",cont);
}
while((strcmp(cont,answer3)==0) || (strcmp(cont,answer4)==0));

printf("*   End of Program  *!");
getch();
clrscr();
return(0);
}
/***********************************************************/
/* This function correct the baseline of the recorded traces */
/* using the pre-trigger part of the curve                   */
/***********************************************************/

void offset (float vector[5000],int points, float trigpos)
{
 int o,p;
 float sum;
 sum=0;


 p=int((points*trigpos/100)-1);
 for (o=1;o<=p;++o)
  sum=sum+vector[o];

 sum=sum/p;

 for (o=1;o<=500;++o)
 {
   vector[o]=vector[o]-sum;

 }

}
/*****************************************************/
/* converts hours minutes seconds into seconds only */
/*****************************************************/

float converttime(int HH, int MM, int SS)
{
 return (HH*3600.0+MM*60.0+SS*1.0);
}
```

8.3 Curriculum Vitae of the author

Name: Markus Clark Scharber

Address: Robert-Stolz-Str. 19/47
             4020 Linz
             Tel.: 0732/656420

Personal data:

Date of birth: 07.11.1971
Birthplace: Salzburg
Marital status: unmarried

Education:

1991-1995	Study at the Johannes Kepler-University Linz, Tech. physics;
Sept.1995 - Jul.1996	continuing my studies at the Napier University Edinburgh, Scotland (Applied physics with Micro-Computing)
12 July 1996	I have been awarded the Degree of Bachelor of Science with first class Honours
Since 01.10.1996	I continue my studies in Linz

Personal Interests

Sports, Scotland

8.4 Publications

During my diploma thesis I attended conferences and summerschools in Obdach (A), Montpellier (F) and Hirschegg (A).
Parts of my work at the Abteilung für Physikalische Chemie have been presented at the ICSM 1998 and have been published in scientific journals. Enclosed a list of conference proceedings and publications can be found.

Time Resolved Photoinduced Electron Spin Resonance Studies on Conjugated Polymer Fullerene Mixtures in Solution;
M .C. Scharber, C. J. Brabec, V. Dyakonov, N. S. Sariciftci
Conference Proceedings ICSM 1998, Montpellier (submitted)

PHOTOEXCITATIONS IN CARBAZOLYL SUBSTITUTED POLYDIACETYLENE (PDA) FULLERENE COMPOSITES
C. Brabec, M. Scharber, H. Johansson, D. Comoretto, G. Dellepiane, I. Moggio, A. Cravino, J.C. Hummelen, N. S. Sariciftci
Conference Proceedings ICSM 1998, Montpellier (submitted)

Studies of Photoinduced Charge Transfer in Conjugated Polymer-Fullerene Composites by Light-Induced ESR,
V. Dyakonov, G. Zoriniants, M. Scharber, C. J. Brabec, R. A. J. Janssen, J. C. Hummelen and N. S. Sariciftci
Conference Proceedings,XII International Winterschool, Kirchberg, Tyrol, Austria 1998, 257

Photoinduced Charge Carriers in Conjugated Polymer-Fullerene Composites Studied with Light-Induced Electron Spin Resonance (LESR)

V. Dyakonov, G. Zoriniants, M. Scharber, C. J. Brabec, R. A. J. Janssen, J. C. Hummelen and N. S. Sariciftci, Phys. Rev. B (in press)